Det Kongelige Danske Videnskabernes Selskab
Matematisk-fysiske Meddelelser, bind **30,** nr. 6

Dan. Mat. Fys. Medd. **30,** no. 6 (1955)

DEDICATED TO PROFESSOR NIELS BOHR ON THE OCCASION OF HIS 70TH BIRTHDAY

A POLARIMETRIC METHOD FOR THICKNESS CONTROL IN THE PRODUCTION OF INTERFERENCE FILTERS

BY

ALFRED HERMANSEN

København 1955
i kommission hos Ejnar Munksgaard

CONTENTS

Printed in Denmark
Bianco Lunos Bogtrykkeri A-S

Introduction.

In a previous paper [*A*] a general theory for interference filters (with two, three, or four reflective systems of layers) has been developed and numerical calculations of $I(\lambda)$, $R(\lambda)$ (i. e. the intensity distribution in transmitted and reflected light) have been carried out in the special case for the reflective systems consisting of silver layers.

The present paper will deal with the problem of measuring the thickness of the different thin layers during the evaporation process.

In a following paper the apparatus used for producing interference filters of a large area (22 × 22 cm) will be described and experimental results for some filters of different type will be given.

The Different Methods of Thickness Control.

In order to make interference filters of different type with optimum properties and with transmission bands at a specified wavelength it is very important to be able to control the thicknesses of the different thin layers during evaporation, especially the dielectric layers.

The thickness of a silver layer (or another absorbent layer) can be determined with sufficient accuracy by measuring the intensity of light *transmitted* through one or more test plates by means of a photocell. The thickness of the silver layers should only be determined with an accuracy better than about 4 per cent. Measurement of the thickness of a dielectric layer deposited on a glass plate or on a silver layer is much more difficult and should for interference filters be determined with an accuracy better than 0.5 per cent.

In 1949 GREENLAND and BILLINGTON [1] indicated an ingenious method for controlling the thickness of the dielectric layer L_{2m} by production of a Fabry-Perot filter $M L_{2m} M$.

By cementing a prism on to the back of the filter blank total reflection is obtained at the lower boundary of the dielectric layer, and the silver-dielectric layers in this way act as a reflection interference filter at oblique incidence (fig. 1, page 5). As we have $R = 1$ at the bottom of the filter, the condition $\sigma \boldsymbol{R} = 1$ ([*A*] 3,22) is nearly satisfied for the *s*-component and a sharp minimum ("absorption line") will appear in a spectroscope. The position of this minimum is determined by the thickness of the dielectric layer. The relation between $\lambda_m^{(s)}$ and $\lambda_m^{(o)}$ (the position of the transmission band at normal incidence) can either be determined experimentally (as done by GREENLAND [1]) or it can, in principle, be calculated by means of a procedure analogous to [*A*] pages 39—42.

This spectroscopic method of control is independent of optical properties or coatings on the "windows" in the vacuum chamber and can be used in the case of a glass bell jar. The measurement of the optical thickness *nd* by this method will depend upon n, as will be shown below.

DUFOUR [2] has controlled the thickness of dielectric layers by intensity measurements of monochromatic light *reflected* from test plates at normal incidence. This method, which has been improved by JACQUINOT and GIACOMO [3], has especially been used in the making of all-dielectric interference filters ([*A*] § 7). At least two test plates are used, one for the low- and the other for the high-index material (see p. 36). This method depends upon coatings on the "windows", but in theory the measurement of *nd* is independent of n.

To make filters of a large area the filter blank has to be rotated during evaporation, but rotation makes it necessary to place test plates far away from the filter blank, and hence it is of importance to find methods which avoid test plates, so that all the thickness measurements of the dielectric layers are carried out on the filter blank itself.

Such a method of control, which has proved valuable, consists in polarimetric measurements of the phase difference

$\Delta = \delta_p - \delta_s$ $\left(\text{and } tg\ \psi = \frac{\varrho_p}{\varrho_s}\right)$ in *reflected* monochromatic light at an oblique angle of incidence (e. g. 75°) [4]. This method of control is particularly well suited for production of filters with two, three, or four silver layers (treated in [*A*] § 3—5); but it can

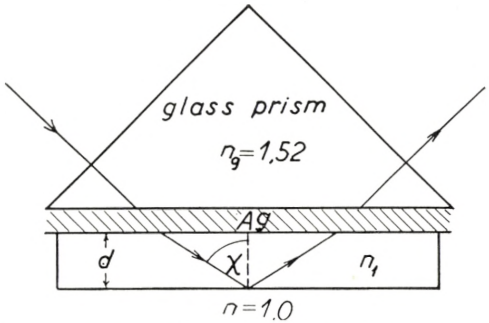

Fig. 1. GREENLAND's method of thickness control.
The silver-dielectric layers act as a reflection interference filter and the narrow absorption band is observed in a spectroscope during evaporation.

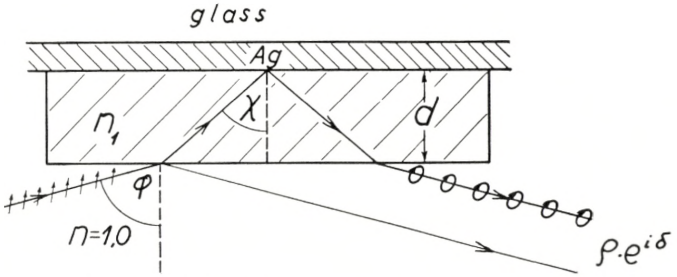

Fig. 2. Polarimetric method of thickness control.
Plane-polarized light (with azimuth about 45°) is reflected from the filter layers and the light (which is elliptically polarized after reflection) is analyzed during evaporation.

also be used for control of all-dielectric filters and for thickness control of reflection interference filters of the HADLEY-DENNISON type.

This method requires two plane windows placed in oblique tubes in the vacuum chamber perpendicularly to the pencil of rays. The method is independent of coatings on the windows, but on the other hand the windows must not be birefringent. Similar to GREENLAND's method the measurement of nd is also here dependent upon n.

Already DRUDE [5] developed formulae which enabled him, from measurements of Δ (and ψ) at oblique incidence, to determine the thickness of very thin dielectric layers (less than 50 Å) on a metal surface. Many years later VAŠIČEK [6] used the same method to determine n and d of thin dielectric layers on a glass base. ROTHEN [7] and ROTHEN and HANSON [8] have used the same method for measurement of dielectric layers as thick as 1—8 λ deposited on a polished steel surface. From their calculations it appeared that the same method could be adapted to control of the thickness of the dielectric layer L_{2m} by production of FABRY-PEROT interference filters $M\,L_{2m}M$. This assumption has been confirmed in recent years in practice in this laboratory [4] and [9].

§ 1. Theory of the Polarimetric Method for Thickness Control.

(Calculation of Δ and ψ)

The problem is:

The FRESNEL factor $r_m = \varrho_m \cdot e^{i\delta_m}$ for a system of m thin layers bounded to vacuum (or air) (fig. 3) is known. To this system is added one more layer consisting of material $m+1$

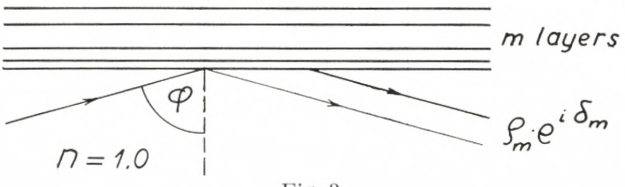

Fig. 3.

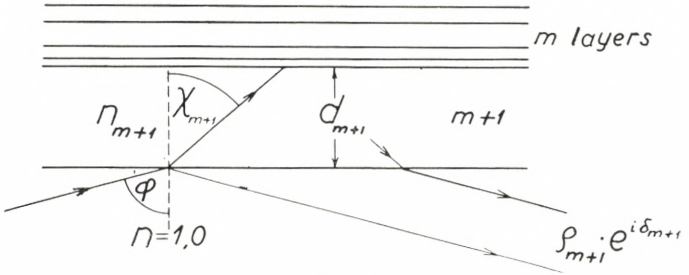

Fig. 4.

(fig. 4), and then $r_{m+1} = \varrho_{m+1} \cdot e^{i\delta_{m+1}}$ for the new system has to be determined.

When r'_{m+1} is the FRESNEL coefficient ([A] 1, 2—3) at the boundary between vacuum and material $m+1$ (fig. 5), the FRESNEL factor $r''_m = \varrho''_m \cdot e^{i\delta''_m}$ in reflection from the system of m

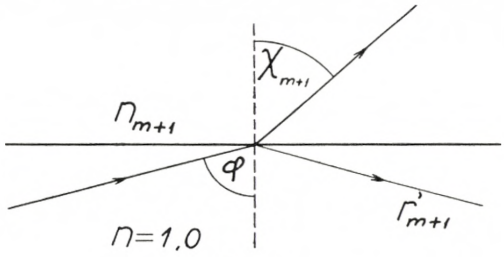

Fig. 5.

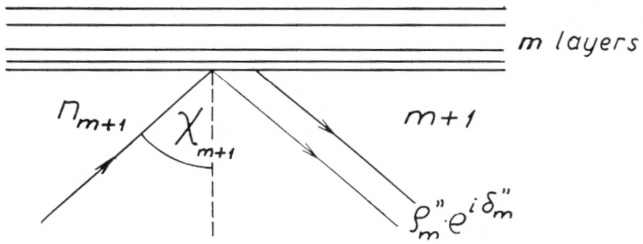

Fig. 6.

layers with material $m+1$ in front (infinite thickness) (fig. 6) is determined from ([A] 2, 7) when $x_m = 0$ is introduced. We obtain

$$r''_m = \varrho''_m \cdot e^{i\delta''_m} = \frac{-r'_{m+1} + \varrho_m \cdot e^{i\delta_m}}{1 - r'_{m+1} \cdot \varrho_m \cdot e^{i\delta_m}}, \qquad (1, 1)$$

and again from ([A] 2, 7) we finally get:

$$r_{m+1} = \varrho_{m+1} \cdot e^{i\delta_{m+1}} = \frac{r'_{m+1} + \varrho''_m \cdot e^{i\delta''_m - ix_{m+1}}}{1 + r'_{m+1} \cdot \varrho''_m \cdot e^{i\delta''_m - ix_{m+1}}} \qquad (1, 2)$$

with

$$x_{m+1} = \frac{360}{\lambda_0} \cdot 2\, d_{m+1} \cdot n_{m+1} \cdot \cos \chi_{m+1} \qquad (1, 3)$$

for the system of $m+1$ layers bounded to vacuum (or air) (fig. 4). λ_0 is the wavelength of the incident plane-polarized light,

which after reflection from the system of thin layers becomes elliptically polarized.

s and p components should be treated separately. The layer $m+1$ added may be absorbent or not; if absorbent also r'_{m+1} and x_{m+1} will be complex numbers. The layer $m+1$ may also be birefringent, in this case $x^{(s)}_{m+1}$ is different from $x^{(p)}_{m+1}$.

The calculation of the observable quantities $\Delta = \delta_p - \delta_s$ and ψ $\left(\operatorname{tg}\psi = \frac{\varrho_p}{\varrho_s}\right)$ can in all cases be carried out *direct from the recurrence formulae* (1, 1—3) *by means of* RYBNER's *tables* [10], when the Fresnel coefficients ([*A*] §1) have first been calculated. If the layer $m+1$ is absorbent (e. g. a silver layer) this procedure will be most convenient. However, if the layer $m+1$ is *not absorbent* (i. e. a dielectric layer) other procedures may be followed.

In this case (1, 1—2) can be written:

$$\varrho''^2_m = 1 - \frac{(1 - r'^2_{m+1})\cdot(1 - \varrho^2_m)}{1 + (r'_{m+1}\cdot\varrho_m)^2 - 2\cdot r'_{m+1}\cdot\varrho_m\cdot\cos\delta_m} \qquad (1,\ 4)$$

$$\varrho^2_{m+1} = 1 - \frac{(1 - r'^2_{m+1})\cdot(1 - \varrho''^2_m)}{1 + (r'_{m+1}\cdot\varrho''_m)^2 + 2\,r'_{m+1}\cdot\varrho''_m\cdot\cos(\delta''_m - x_{m+1})} \qquad (1,\ 5)$$

$$\operatorname{tg}\delta''_m = \frac{\varrho_m\cdot(1 - r'^2_{m+1})\cdot\sin\delta_m}{-r'_{m+1}\cdot(1+\varrho^2_m) + \varrho_m\cdot(1 + r'^2_{m+1})\cdot\cos\delta_m} \qquad (1,\ 6)$$

$$\operatorname{tg}\delta_{m+1} = \frac{\varrho''_m\cdot(1 - r'^2_{m+1})\cdot\sin(\delta''_m - x_{m+1})}{r'_{m+1}\cdot(1+\varrho''^2_m) + \varrho''_m\cdot(1 + r'^2_{m+1})\cdot\cos(\delta''_m - x_{m+1})}, \qquad (1,\ 7)$$

and the derivative $\dfrac{\partial(\delta_{m+1})}{\partial(x_{m+1})}$ can in this case be expressed by

$$-\frac{\partial(\delta_{m+1})}{\partial(x_{m+1})} = \left.\begin{array}{l} \\ \dfrac{\varrho''_m\cdot(1 - r'^2_{m+1})\cdot(\varrho''_m(1 + r'^2_{m+1}) + r'_{m+1}\cdot(1+\varrho''^2_m)\cdot\cos(\delta''_m - x_{m+1}))}{(r'_{m+1}\cdot(1+\varrho''^2_m) + \varrho''_m\cdot(1+r^2_{m+1})\cdot\cos(\delta''_m - x_{m+1}))^2} \cdot \\ \qquad + (\varrho''_m\cdot(1 - r'^2_{m+1})\cdot\sin(\delta''_m - x_{m+1}))^2 \end{array}\right\} \qquad (1,\ 8)$$

Another method to calculate Δ (and ψ) as a function of nd when $m+1$ is a dielectric layer, consists in inversion of complex

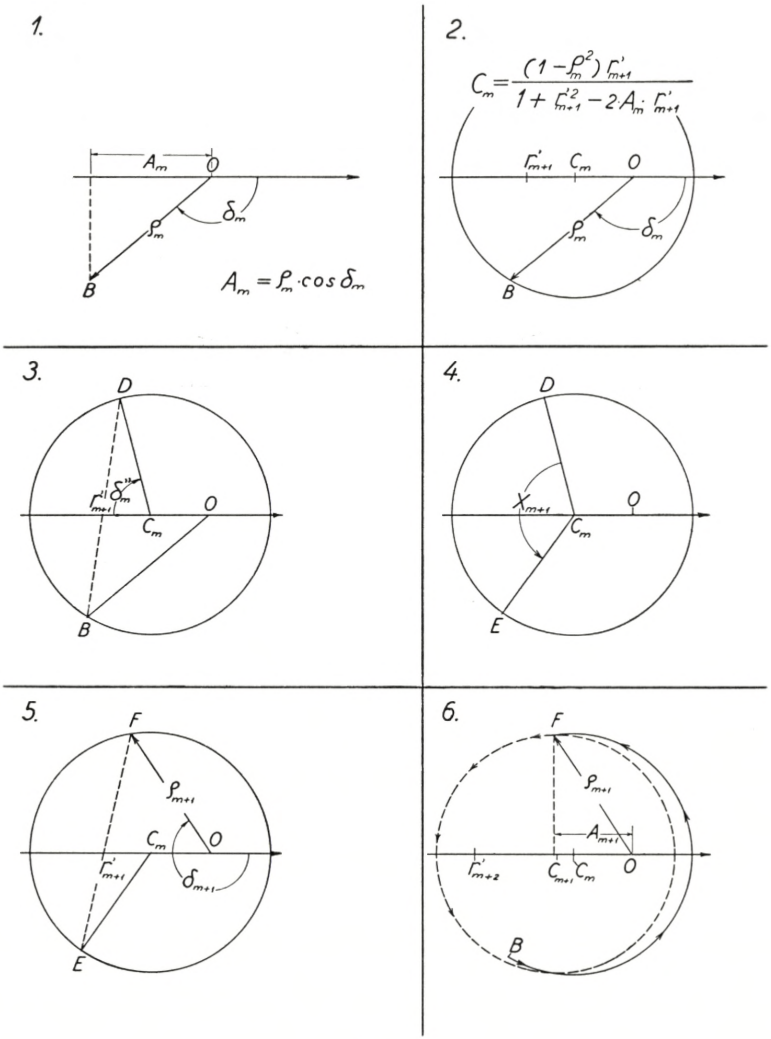

Fig. 7.

1. The complex number (ϱ_m, δ_m) is plotted (point B, clockwise return).
2. The centre $C_m = \dfrac{r'_{m+1}(1-\varrho_m^2)}{1 + r'^2_{m+1} - 2\, r'_{m+1} \cdot \varrho_m \cdot \cos \delta_m}$ is calculated, and a circle is drawn through B with C_m as centre.
3. The point B is inverted to point D (with $(r'_{m+1}, 0)$ as inversion centre).
4. The angle x_{m+1} is plotted (counterclockwise return).
5. The point E is inverted to point F, which is equal to $(\varrho_{m+1}, \delta_{m+1})$.
6. If to the system is added a new dielectric layer $m + 2$ with another index of refraction n_{m+2}, a new centre C_{m+1} is calculated, a new circle is drawn through F (broken line), and the procedure is repeated.

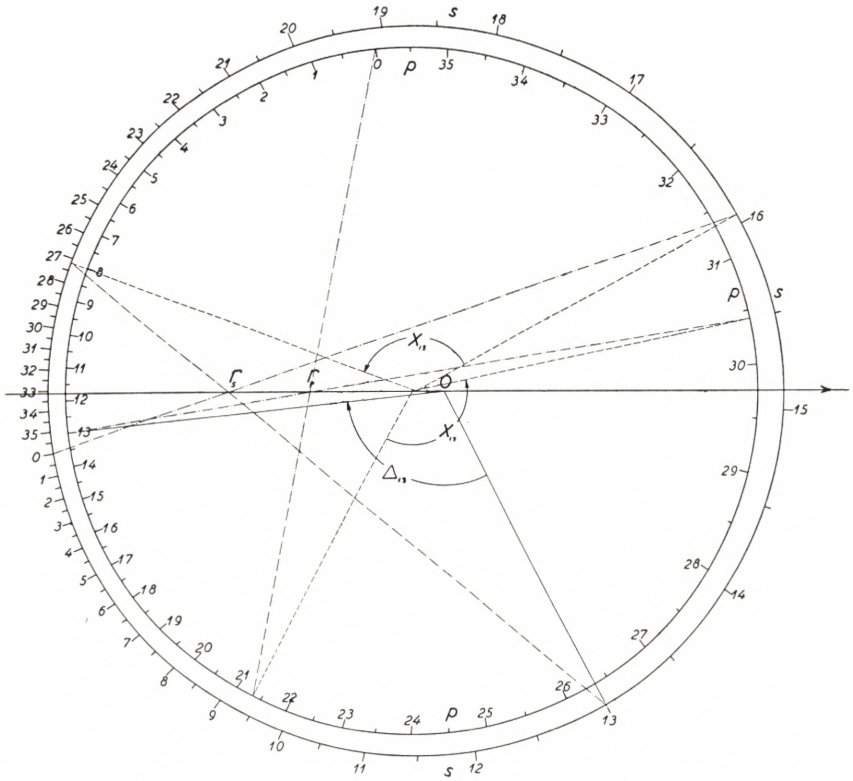

Fig. 8. Graphical calculation of a (Δ, x) curve for a fluoride layer with index of refraction $n = 1.29$ deposited upon a silver layer with $\nu - i\varkappa = 0.1 - i\,3.5$ and thickness $t = 350$ Å. The numbers on the s and the p circles correspond to the same values of x with ten degrees' interval (e. g. 13 corresponds to $x = 130°$). The corresponding (Δ, nd) curve is shown in fig. 28 *p.* 31, unbroken line. In the same way also $\frac{\varrho_p}{\varrho_s} = \operatorname{tg}\psi$ can be derived from fig. 8. Angle of incidence $\varphi = 75°$.

numbers. The different steps in this graphical method (which enable us direct to determine $(\varrho_{m+1}, \delta_{m+1})$ from (ϱ_m, δ_m)) are shown in fig. 7 (1—6). The procedure employed in fig. 7 is a modification of a method indicated by COTTON [11].

In fig. 8 is shown the graphical procedure in the calculation of a (Δ, x) curve for a fluoride layer with a silver layer at the bottom. When a polar coordinathograph for plotting complex numbers (ϱ, δ) is used in the graphical method, the deviations in Δ from the exactly calculated values will be less than $\frac{1°}{3}$, which will be sufficiently accurate in the case of $\varphi = 75°$.

All the (Δ, nd) curves shown in the following figures have been calculated by means of this convenient graphical method. (Δ_0, ψ_0) for the bottom silver layers are calculated direct from (1, 1—2) by means of RYBNER's tables [10].

§ 2. The Accuracy and General Trend of the Polarimetric Method.

In fig. 9 is shown (Δ, nd) curves corresponding to a fluoride layer with $n = 1.28$ (quickly evaporated MgF_2) deposited upon

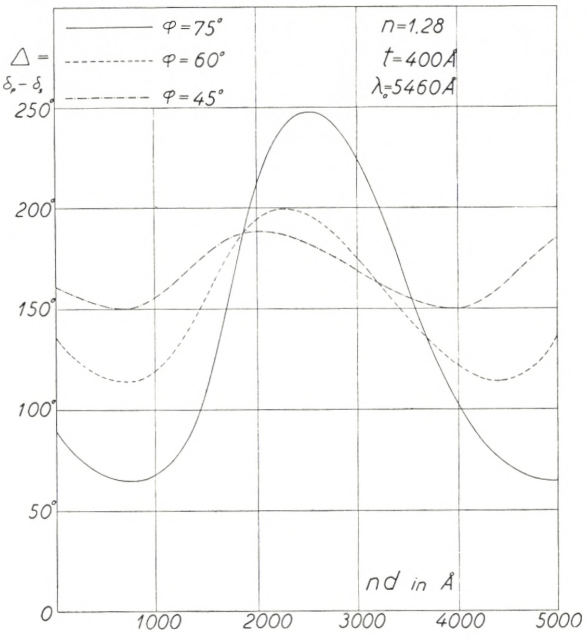

Fig. 9.

a silver layer with $t = 400$ Å. The three curves correspond to different angles of incidence $\varphi = 45°$, $60°$ and $75°$.

Δ is a periodic function of x with 360° as the period or as a function of nd with the period $\frac{\lambda_0}{2 \cos \chi}$, where λ_0 is the wavelength of the polarimeter light and no birefringence is assumed.

The steepness $\frac{\partial \Delta}{\partial (nd)}$ af the curves increases rapidly with increasing angle of incidence.

If n changes its value during evaporation from n to $n + \Delta n$, this gives rise to an uncertainty in the determination of nd and thus also to a change in the position of the transmission band λ_1 for the filter we wish to make. If the evaporation of the dielectric material is stopped at a value of Δ corresponding closely to one whole period ($\Delta \simeq \Delta_0$), the uncertainty in nd can be determined from the derivative of

$$nd = \frac{\lambda_0}{2\sqrt{1 - \frac{\sin^2 \varphi}{n^2}}}.$$

We get

$$\Delta(nd) = \frac{\lambda_0 \cdot \sin^2 \chi}{2\, n \cdot \cos^3 \chi} \cdot \Delta n, \qquad (2,\ 1)$$

and as one whole period on the (Δ, nd) curve corresponds to an interference filter of the second order, the uncertainty $\Delta \lambda_1$, in the position of the transmission band λ_1, will have the same value as $\Delta(nd)$. In Table 1 $\Delta \lambda_1$ is calculated correspondingly to $\lambda_0 =$ 5460 Å when n decreases to $n - 0.01$ during the total period of evaporation. The corresponding uncertainty of GREENLAND's method of control is added in the table. If a change in birefringence $n_p - n_s$ takes place during evaporation, this will give an additional uncertainty for the polarimetric method in contrast to GREENLAND's method, where only the s component is used. In column 4 $\frac{\partial(\Delta)}{\partial(nd)}$ is given for the steep part of the curves in the neighbourhood of $x = 360°$ measured in degrees per Ångström and in column 5,

TABLE 1. ($\Delta\lambda_1$ corresponds to $\Delta n = 0.01$).

	$\cos \chi$ ($n = 1.28$)	$\Delta\lambda_1$ ($n = 1.28$)	$\frac{\partial \Delta}{\partial (nd)}$ ($n = 1.28$)	$\Delta\lambda_1$ ($n = 2.36$)
Greenland's method:	0.54500	92.6 Å		3.4 Å
Polarimetric method:				
$\varphi = 75°$	0.65615	43.3 —	0.090 degree / Å	2.6 —
60°	0.73637	24.6 —	0.045 —	2.0 —
45°	0.83356	11.3 —	0.022 —	1.2 —

$\Delta\,\lambda_1$ is calculated for a high-index layer $n = 2.36$ (ZnS). $\Delta\,n = 0.01$ will in this case give a negligible change in λ_1.

In what follows $\varphi = 75°$ is employed; however, when a photoelectric method is used, $\varphi = 60°$ would give sufficient accuracy.

In fig. 10 (Δ, nd) curves are shown for different values of n, all calculated for $\varphi = 75°$ and with the same silver layer as

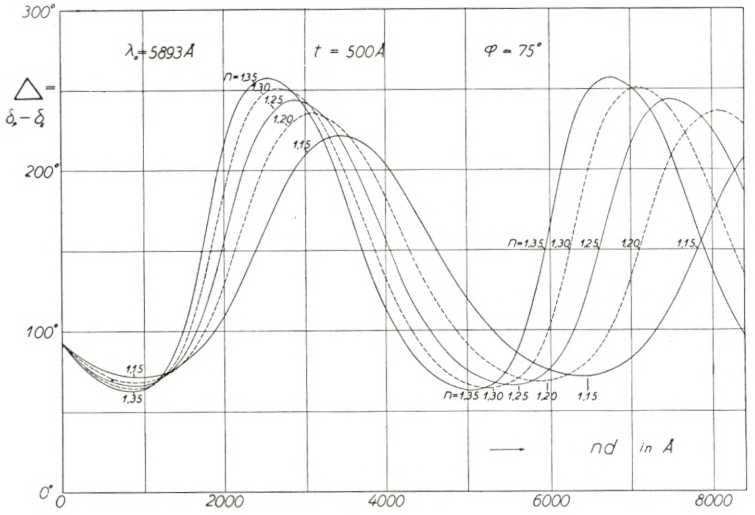

Fig. 10.

"bottom" layer. Fig. 10 shows that even if a dielectric material was available with n as low as 1.15, the polarimetric method of thickness control would give sufficient accuracy. From fig. 10 we are further able to calculate the uncertainty of nd caused by a change in n for all values of nd.

Fig. 10 shows that as n increases $\Delta_{\min}$ will decrease and $\Delta_{\max}$ increase. $\Delta_{\max} - \Delta_{\min}$ (which can be determined during evaporation and which, as calculations show, is independent of small changes in (Δ_0, ψ_0) for the silver layer) determine n of the dielectric layer. If desired, the values of $\Delta_{\max}$ and $\Delta_{\min}$ can be exactly calculated by means of (1, 8) ($n_s d$ is determined in such a way that $\dfrac{\partial(\delta_s)}{\partial(n_s d)} - \dfrac{\partial(\delta_p)}{\partial(n_s d)} = 0$). In Table 2 a few calculations of this type are added. $\varphi = 75°$ $\nu - i\varkappa = 0.1 - i\,3.6$ and $t = 400$ Å for the silver layer.

TABLE 2.

n	Δ_{min}	Δ_{max}	$\Delta_{max} - \Delta_{min}$
1.25	65°.71	243°.28	177°.57
1.30	63.97	250.76	186.79
1.35	62.60	256.61	194.01
1.40	61.46	261.27	199.81

(no birefringence is assumed)

TABLE 3. $\varphi = 75°$.

n	$\cos \chi$	$-r_s$	$-r_p$	
1.15	0.54269	0.41371	0.29161	
...				
1.20	.59336	.46682	.31283	
1.21	.60227	.47584	.31570	
1.22	.61086	.48446	.31846	
1.23	.61910	.49266	.32082	
1.24	.62706	.50052	.32291	
1.25	.63472	.50805	.32476	
1.26	.64211	.51526	.32637	
1.27	.64924	.52218	.32777	
1.28	.65615	.52886	.32899	
1.29	.66282	.53527	.33003	
1.30	.66927	.54145	.33089	
1.31	.67551	.54741	.33164	
1.32	.68155	.55317	.33221	
1.33	.68742	.55874	.33266	
1.34	.69310	.56412	.33299	
1.35	.69861	.56932	.33320	
1.36	.70396	.57438	.33331	
1.37	.70915	.57928	.33332	
1.38	.71420	.58403	.33325	
1.39	.71910	.58864	.33307	
1.40	.72386	.59312	.33281	
1.518	.77132	.63788	.32514	(glass)
2.36	.91240	.78540	.19799	(ZnS)

In Table 3 (r_s, r_p) are calculated for $\varphi = 75°$ and different values of n (from ([A] 1, 1—3)).

For values of nd, where Δ is near a minimum or a maximum, it would be impossible to determine nd with sufficient accuracy.

However, the wavelength λ_0 of the polarimeter light can be changed which alters the position of minimum and maximum on the (Δ, nd) curve, and in this way all values of nd can be controlled with sufficient accuracy on a steep part of a (Δ, nd) curve. (Figs. 27—28, p. 31).

Before the detailed procedure is given which enables us to calculate a (Δ, nd) curve which best fits to the experimental results, it should be emphasized that nd for filters $M\,L_{2m}M$ of the second (or higher orders) ($m \geqslant 2$) can be determined in the simplest manner when the wavelength λ_0 for the polarimeter light is chosen in such a way that x is near 360°, i. e. $\lambda_0 = 2\,dn \cdot \cos\chi$ (or $\lambda_0 = dn \cdot \cos\chi$) (for $\varphi = 75°$ $\lambda_2 = 5050$ Å corresponds to $\lambda_0 = 5461$ Å).

In this case the nd determination will be independent of Δ_0 (the value of Δ when the evaporation of the dielectric layer is started), and without any knowledge of the theory the polarimetric method of control can be used empirically also for compound filters with three or four silver layers (and two or three dielectric layers) and even with a glass bell jar (free from strains) as vacuum chamber.

λ_0 can be altered in practice by means of interference filters in connection with a tungsten band-lamp.

As a (Δ, nd) curve with a silver layer as bottom layer only shows a small dependence upon t (for $t > 350$ Å), an empirical (Δ, nd) curve can be determined and also filters of the first order controlled.

However, theoretical calculations of (Δ, nd) curves or (Δ, λ_m) curves, which best fit the experimental results, will be of great value for determining the physical properties of evaporated thin films and for more complicated filters, such as $M\,L'H_2L'M$, or at all-dielectric filters empirical determination of the (Δ, nd) curve would be much too complicated.

This procedure is more complicated, as previously assumed, because of the following important experimental facts:

1. $\varkappa$ for a silver layer of thickness $t \simeq 400$—500 Å is different from $\varkappa$ for an opaque silver layer.

TABLE 4. $\Delta = \delta_p - \delta_s$.

$\varkappa$ \ v	0.0	0.1	0.2
2.0	63.28	63.29	63.33
2.1	65.34	65.35	65.40
2.2	67.37	67.39	67.43
2.3	69.37	69.38	69.44
2.4	71.33	71.35	71.40
2.5	73.26	73.28	73.33
2.6	75.15	75.17	75.23
2.7	77.00	77.02	77.08
2.8	78.82	78.84	78.89
2.9	80.59	80.61	80.67
3.0	82.33	82.34	82.40
3.1	84.02	84.04	84.10
3.2	85.68	85.70	85.76
3.3	87.29	87.31	87.37
3.4	88.87	88.89	88.95
3.5	90.41	90.43	90.49
3.6	91.91	91.93	91.99
3.7	93.38	93.40	93.45
3.8	94.81	94.83	94.88
3.9	96.20	96.22	96.27
4.0	97.56	97.58	97.63
4.1	98.89	98.90	98.95
4.2	100.18	100.19	100.24
4.3	101.44	101.45	101.50
4.4	102.66	102.68	102.73
4.5	103.86	103.88	103.92
4.6	105.03	105.04	105.09
4.7	106.17	106.18	106.22
4.8	107.28	107.29	107.33
4.9	108.36	108.37	108.41
5.0	109.41	109.42	109.46

TABLE 5. $\operatorname{tg}\psi = \varrho_p/\varrho_s$.

$\varkappa$ \ v	0.1	0.2
2.0	0.9644	0.9301
2.1	.9649	.9310
2.2	.9654	.9320
2.3	.9660	.9331
2.4	.9666	.9343
2.5	.9672	.9355
2.6	.9679	.9367
2.7	.9685	.9380
2.8	.9692	.9393
2.9	.9698	.9406
3.0	.9705	.9419
3.1	.9712	.9432
3.2	.9718	.9445
3.3	.9725	.9458
3.4	.9732	.9471
3.5	.9738	.9483
3.6	.9744	.9495
3.7	.9751	.9507
3.8	.9757	.9519
3.9	.9763	.9531
4.0	.9768	.9543
4.1	.9774	.9554
4.2	.9780	.9565
4.3	.9786	.9576
4.4	.9791	.9586
4.5	.9796	.9596
4.6	.9801	.9606
4.7	.9806	.9616
4.8	.9811	.9625
4.9	.9815	.9634
5.0	.9820	.9643

2. $n^{(v)}$ (n measured in the vacuum container) for a low index layer is different from $n^{(A)}$ (n measured in air) when the material is quickly evaporated. (For MgF_2 we have $n^{(v)} = 1.28$ and $n^{(A)} = 1.365$).

3. A fluoride layer quickly evaporated shows a small birefringence

$$n_p^{(v)} > n_s^{(v)} \quad (\text{for } MgF_2 \quad n_p - n_s \simeq 0.005).$$

For ZnS and other high index layers we have $n^{(v)} = n^{(A)}$.

TABLE 6. ϱ_s.

$\varkappa$ \ ν	0.1	0.2
2.0	0.99073	0.98160
2.1	.99135	.98283
2.2	.99193	.98396
2.3	.99245	.98499
2.4	.99293	.98594
2.5	.99337	.98681
2.6	.99377	.98761
2.7	.99414	.98835
2.8	.99448	.98903
2.9	.99480	.98965
3.0	.99509	.99022
3.1	.99535	.99075
3.2	.99560	.99124
3.3	.99583	.99170
3.4	.99605	.99212
3.5	.99624	.99251
3.6	.99642	.99288
3.7	.99659	.99322
3.8	.99675	.99354
3.9	.99691	.99383
4.0	.99705	.99411
4.1	.99718	.99436
4.2	.99730	.99461
4.3	.99741	.99484
4.4	.99752	.99505
4.5	.99762	.99525
4.6	.99773	.99545
4.7	.99780	.99563
4.8	.99789	.99579
4.9	.99797	.99595
5.0	.99805	.99611

TABLE 7. $180 - \delta_s$ ($\varphi = 75°$).

$\varkappa$ \ ν	0.0	0.1	0.2
2.0	13.29	13.27	13.22
2.1	12.78	12.76	12.71
2.2	12.30	12.28	12.23
2.3	11.85	11.83	11.79
2.4	11.43	11.41	11.37
2.5	11.03	11.02	10.98
2.6	10.66	10.65	10.62
2.7	10.31	10.30	10.27
2.8	9.99	9.98	9.95
2.9	9.68	9.67	9.64
3.0	9.39	9.38	9.36
3.1	9.12	9.11	9.08
3.2	8.86	8.85	8.83
3.3	8.61	8.60	8.58
3.4	8.38	8.37	8.35
3.5	8.16	8.15	8.13
3.6	7.94	7.94	7.92
3.7	7.74	7.74	7.72
3.8	7.55	7.55	7.54
3.9	7.37	7.37	7.36
4.0	7.20	7.19	7.18
4.1	7.03	7.03	7.02
4.2	6.87	6.87	6.86
4.3	7.72	6.72	6.71
4.4	6.58	6.57	6.56
4.5	6.44	6.43	6.43
4.6	6.30	6.30	6.29
4.7	6.17	6.17	6.16
4.8	6.05	6.05	6.04
4.9	5.93	5.93	5.92
5.0	5.82	5.82	5.81

§ 3. Determination of (ϱ_s, δ_s) for a Silver Layer.

To be able to calculate a (Δ, nd) curve it is necessary to know not only (Δ_0, ψ_0) $\left(\Delta_0 = \delta_p - \delta_s;\ \operatorname{tg}\psi_0 = \frac{\varrho_p}{\varrho_s}\right)$, but also (ϱ_s, δ_s) for the silver layer first evaporated.

The first step will be to calculate tables of $\left(\Delta, \frac{\varrho_p}{\varrho_s}\right)$ and (ϱ_s, δ_s)

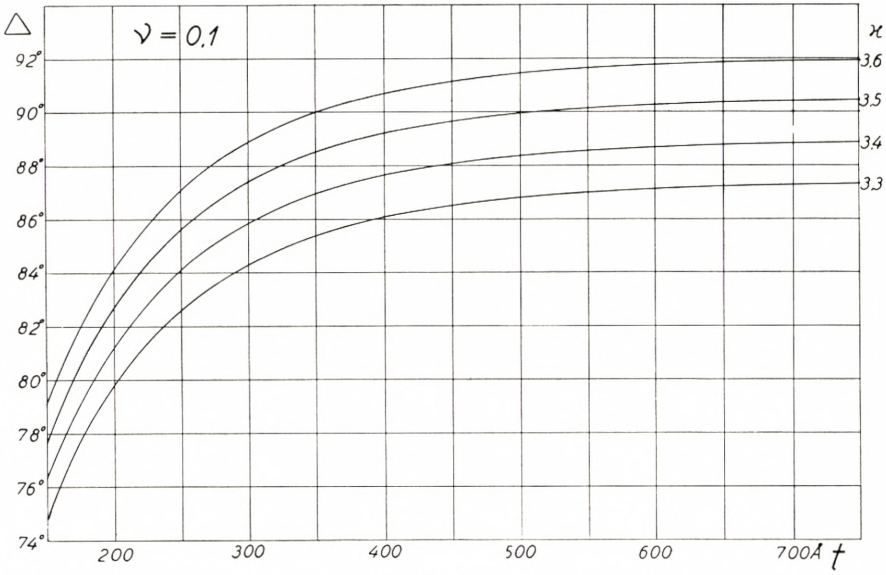
Δ
ν = 0,1
92°
90°
88°
86°
84°
82°
80°
78°
76°
74°
200
300
400
500
600
700Å
t
x
3,6
3,5
3,4
3,3

Fig. 11.

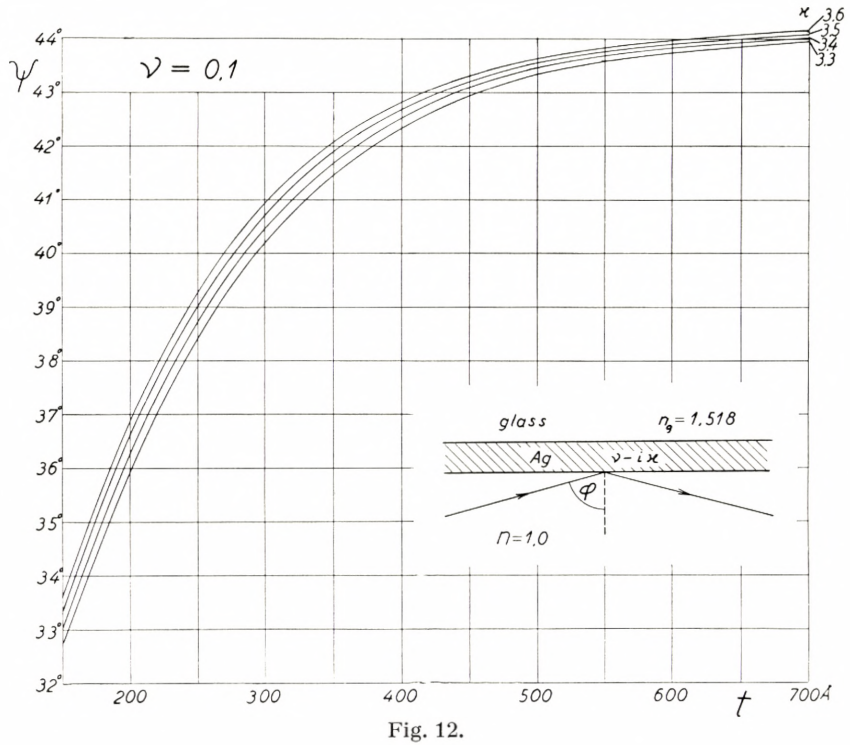
Ψ
ν = 0,1
44°
43°
42°
41°
40°
39°
38°
37°
36°
35°
34°
33°
32°
200
300
400
500
600
700Å
t
x
3,6
3,5
3,4
3,3
glass
$n_g = 1,518$
Ag
ν - i x
φ
n=1,0

Fig. 12.

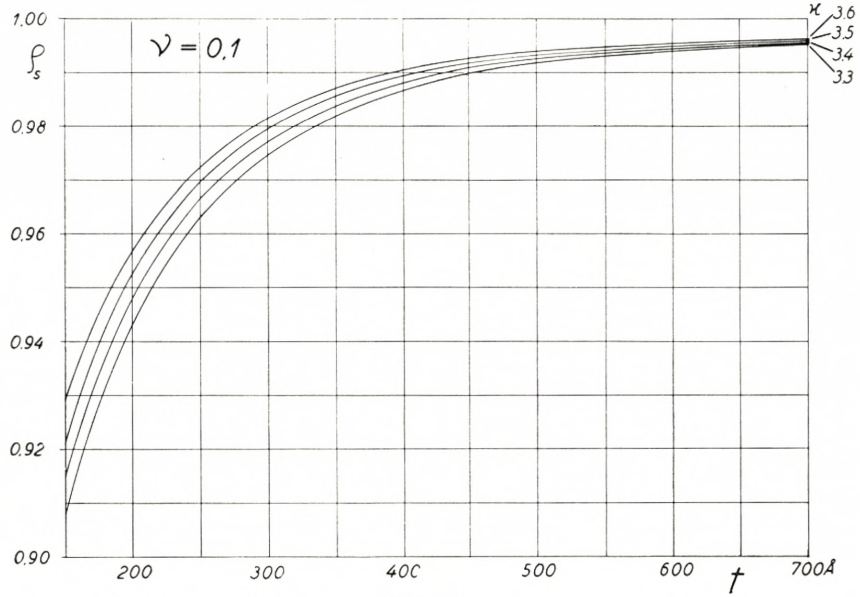
1,00
ρ_s
0,98
0,96
0,94
0,92
0,90
$\nu = 0,1$
$\varkappa$
3,6
3,5
3,4
3,3
200
300
400
500
600
700Å
t

Fig. 13.

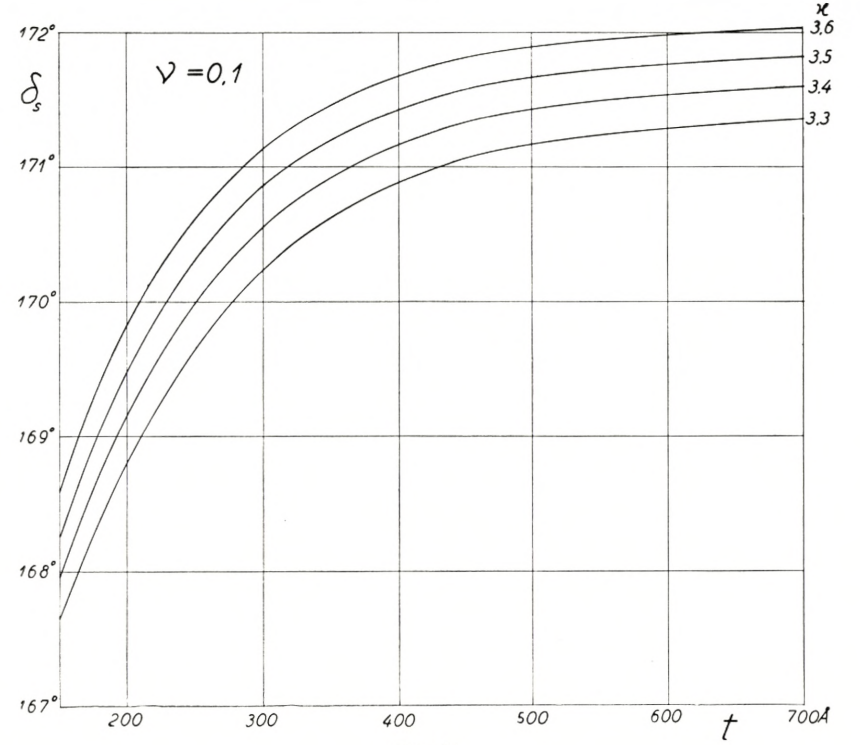
172°
δ_s
171°
170°
169°
168°
167°
$\nu = 0,1$
$\varkappa$
3,6
3,5
3,4
3,3
200
300
400
500
600
700Å
t

Fig. 14.

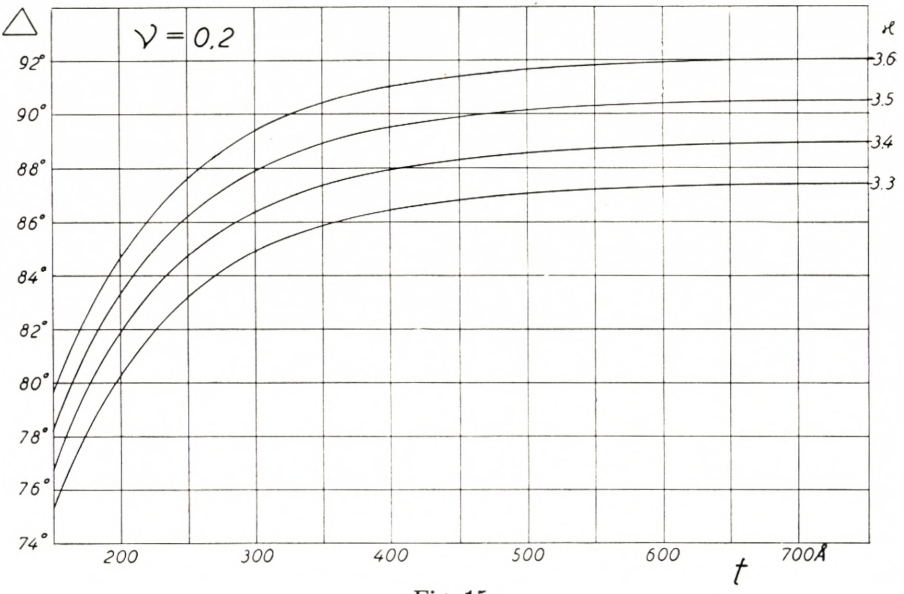
Δ
ν = 0,2
92°
90°
88°
86°
84°
82°
80°
78°
76°
74°
200
300
400
500
600
700Å
t
κ
3.6
3.5
3.4
3.3

Fig. 15.

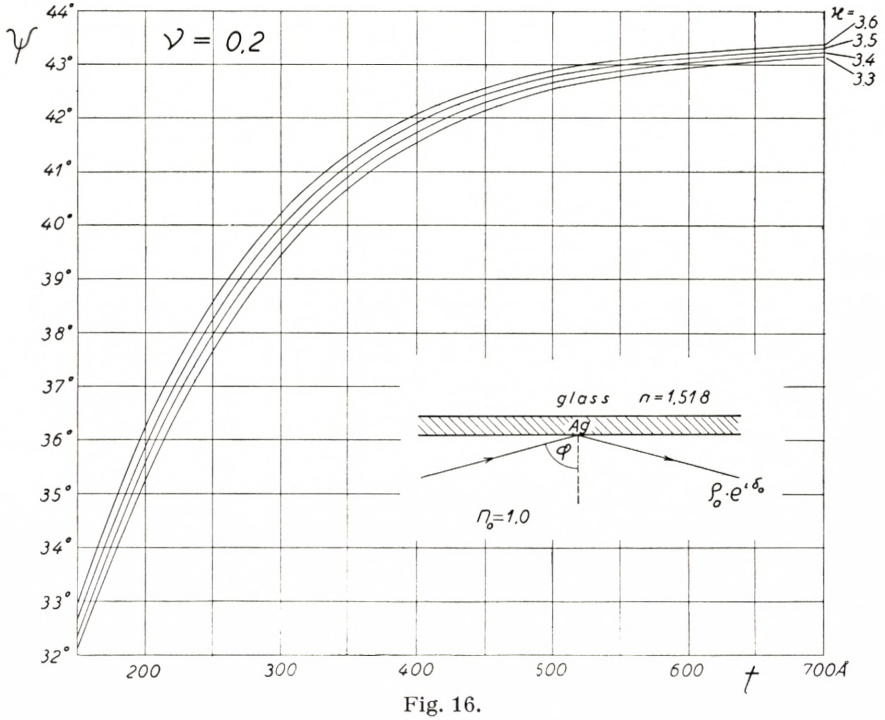
ψ
ν = 0,2
44°
43°
42°
41°
40°
39°
38°
37°
36°
35°
34°
33°
32°
200
300
400
500
600
700Å
t
κ =
3.6
3.5
3.4
3.3
glass n=1,518
Ag
φ
$\rho_0 \cdot e^{i\delta_0}$
n_0=1.0

Fig. 16.

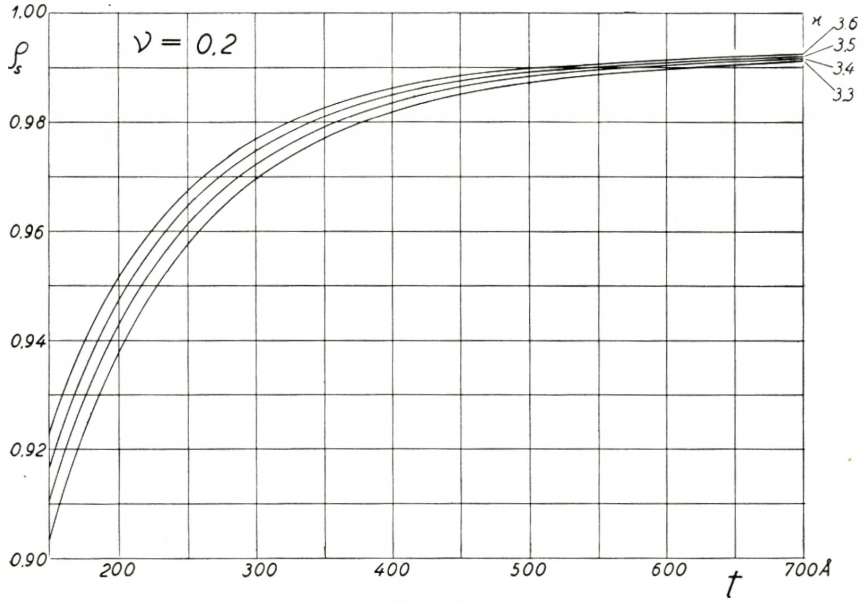
1.00
ρ_s
$\nu = 0.2$
0.98
0.96
0.94
0.92
0.90
200
300
400
500
600
700Å
t
x
3.6
3.5
3.4
3.3

Fig. 17.

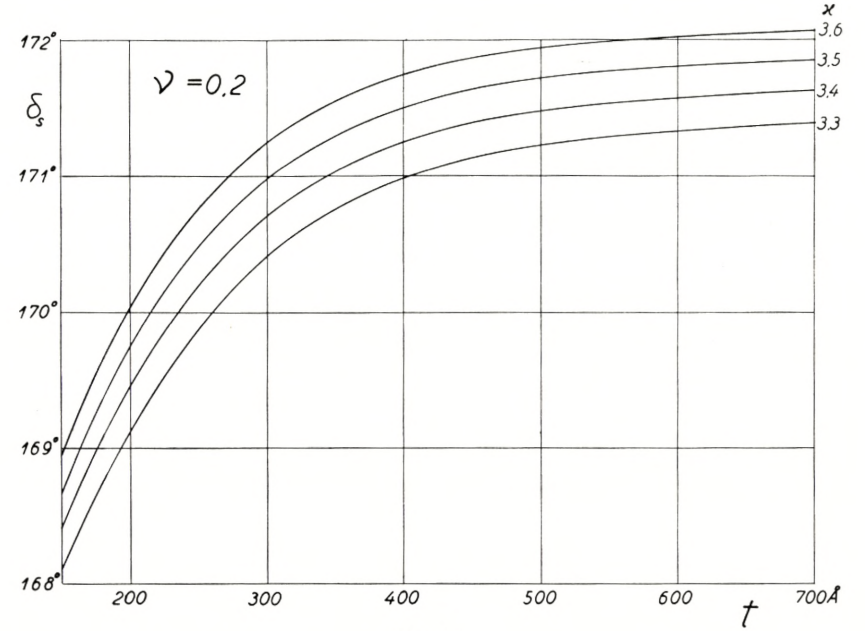
172°
δ_s
$\nu = 0.2$
171°
170°
169°
168°
200
300
400
500
600
700Å
t
x
3.6
3.5
3.4
3.3

Fig. 18.

for an opaque silver layer at $\varphi = 75^\circ$ as a function of $\nu - i\varkappa$. The results of such calculations (carried out by means of ([A] 1, 12—13) are given in Tables 4—7.

The next step will be to calculate the same quantities for different thicknesses t of a silver layer and also for different values of $\nu - i\varkappa$ by means of (1, 1—3). This has been done only for values of $\varkappa$ in the neighbourhood of $\lambda_0 = 5461$ Å, the results being shown in the figs. 11—14 for $\nu = 0.1$ and in the figs. 15—18 for $\nu = 0.2$.

Now the most obvious method would be first to determine $\nu - i\varkappa$ by means of Tables 4—5 from measurements of (Δ_0, ψ_0) for an opaque silver layer. However, experiments show that when the thickness t of a silver layer is increased, Δ reaches a maximum for some definite thickness $t_0 \simeq 450$ Å and then decreases, which according to fig. 11 and fig. 15 means that $\varkappa$ reaches a maximum for $t < t_0$.

As only two observable quantities (Δ_0, ψ_0) are available, we may assume a definite value for ν; when this is done, $\varkappa$ and t can be determined from figs. 11—12 and figs. 15—16. (As a first approximation ν determined for an opaque silver layer can be used). When $\varkappa$ and t are determined for the silver layer, (ϱ_s, δ_s) can be determined from figs. 13—14 and figs. 17—18. It should be emphasized that (ϱ_s, δ_s) in contrast to (ϱ_p, δ_p) only shows a small dependence upon ν and $\varkappa$.

As an example of the above procedure the following experimental results should be given in Table 8.

The measurements are carried out just after evaporation of the layer. The thickness of a silver layer is controlled by transmission measurements at test plates (placed perpendicularly above the evaporation source for silver). A silver layer of thickness $t' = 200$—250 Å is evaporated in one step (only one test plate used) but a silver layer of thickness $t'' = 400$—500 Å is evaporated in two or three steps (two or three test plates are used placed in position in succession). In this way a definite value of $\frac{t''}{t'}$ can be obtained (by means of a photocell). When the current from the photocell is the same for the test plates, we should in theory have $t_2 = 2\,t_1$; $t_3 = 3\,t_1$, etc. in Table 8.

From the measurements it seems as if ν is near 0.1; however,

not until measurements of I_{max} and W_2 for the finished filter have been made, (after the filter has been removed from the vacuum chamber) is it possible to determine ν.

$\varkappa$ depends upon the speed of evaporation, but seems to be independent of the pressure when this is below 10^{-4} mm *Hg*.

TABLE 8. (The transmission through each of the test plates is the same).

Testplate no.	Δ	ψ	$\nu = 0.1$				$\nu = 0.2$			
			t	$\varkappa$	ϱ_s	δ_s	t	$\varkappa$	ϱ_s	δ_s
1	82°80	37°1	210 Å	3.46	0.955	169.54	236 Å	3.32	0.954	169.74
2	90.53	42.5	380	3.60	0.989	171.60	423	3.55	0.987	171.70
3	90.40	43.6	504	3.53	0.993	171.74				
4	90.00	44.0	650	3.48	0.995	171.75				
5	88.74	—		3.40						
6	87.80	—		3.33						
7	87.10	—		3.29						
8	86.40	—		3.24						

For a wavelength λ_0' near 5461 Å figs. 11—18 can still be used if the t-scales are transformed to $t' = t \cdot \frac{\lambda_0'}{5461}$.

§ 4. Determination of n_s and n_p.

When a FABRY-PEROT filter of higher order (e. g. $M\,L_{10}M$) is produced, Δ_{min} and Δ_{max} for several periods of the Δ curve can be measured during evaporation.

Experiments for cryolite and MgF_2 both quickly evaporated now show that small deviations from periodicity are present. We have $\Delta_{min_1} > \Delta_{min_2} > \Delta_{min_3} \ldots$ and $\Delta_{max_1} > \Delta_{max_2} > \Delta_{max_3} \ldots$, which indicates that the evaporated layer is birefringent and that $n_p > n_s$. The film acts as a uniaxial crystal with its optic axis normal to the film. When n_0 is the ordinary and n_e the extraordinary index we have according to BORN [12] or BILLINGS [13]:

$$n_0 = n_s \qquad (4,\ 1)$$

and

$$n_e = \frac{n_p \cdot \sin \chi_p}{\sqrt{1 - \left(\frac{n_p}{n_s}\right)^2 \cos^2 \chi_p}}. \qquad (4,\ 2)$$

(χ_p is determined by $n_p \sin \chi_p = \sin \varphi$).

When birefringence is present, (δ_p, $n_s d$) and (δ_s, $n_s d$) curves must first be constructed separately, and next $\Delta\,(n_s d)$ can be calculated from these curves.

This procedure is illustrated in fig. 19 calculated for $n_s = 1.28$ and $n_p = 1.29$. By means of the p-scale (of $n_s d$) above and the s-scale (of $n_s d$) below in fig. 19 the corresponding (Δ, $n_s d$) curve is constructed in fig. 20 (for $n_s d < 8000$ Å unbroken line and for 8000 Å $< n_s d < 16000$ Å broken line).

As r_p only varies slowly with n (Table 3), fig. 19 can still be used for another value of $n_p = n_p'$ if the p scale (above) is transformed to

$$(n_s d)' = n_s d \cdot \frac{n_p' \cdot \cos \chi_p'}{n_p \cdot \cos \chi_p}. \qquad (4,\ 3)$$

For MgF_2 we have $n_p - n_s \simeq 0.005$. ($n_e - n_0 \simeq 0.009$).

From measurements of $\Delta_{\min_1}$, $\Delta_{\min_2}$ ... and $\Delta_{\max_1}$, $\Delta_{\max_2}$ ... during evaporation it should be possible to determine $n_s^{(v)}$ and $n_p^{(v)}$ (v means measured in vacuum), and from these values and from $\left(\Delta_0, \frac{\varrho_p}{\varrho_s}\right)$ and (ϱ_s,δ_s) for the silver layer the (Δ, $n_s d$) curve can be constructed.

As mentioned above, a great change in n for MgF_2 takes place when air (and H_2O) is admitted to the vacuum chamber and this change in n from $n^{(v)}$ ($= n_s^{(v)}$) to $n^{(A)}$ must be taken into account when we desire to make an interference filter with transmission band at $\lambda_m^{(A)}$ (at normal incidence).

We have ([A] 3, 8)

$$m \cdot \lambda_m^{(A)} = 2\, d n^{(A)} + Z\,(\lambda_m^{(A)},\ n^{(A)}). \qquad (4,\ 4)$$

($Z\,(\lambda_m^{(A)},\ n^{(A)})$ can be determined by means of ([A] fig. 8)), and the evaporation has to be stopped at a value of Δ corresponding to

$$n_s^{(v)} d = \frac{n_s^{(v)}}{2\, n^{(A)}} \cdot (m \cdot \lambda_m^{(A)} - Z\,(\lambda_m^{(A)},\ n^{(A)})). \qquad (4,\ 5)$$

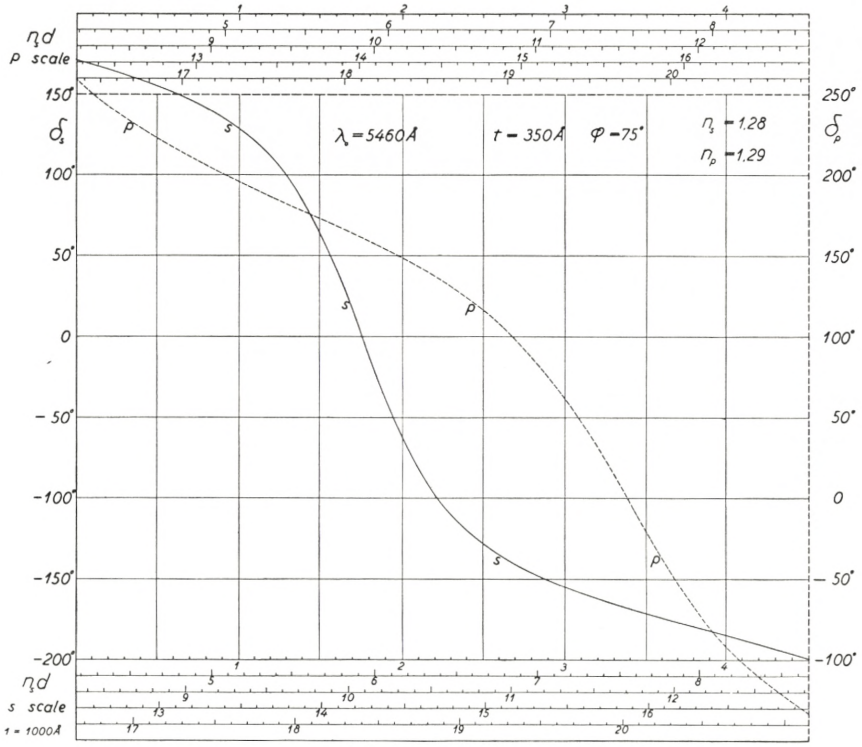
$\eta_1 d$
p scale
δ_s
δ_p
$\lambda_0 = 5460\,Å$
$t = 350\,Å$
$\varphi = 75°$
$n_1 = 1.28$
$n_2 = 1.29$
p
s
150°
100°
50°
0
− 50°
−100°
−150°
−200°
250°
200°
150°
100°
50°
0
− 50°
−100°
$\eta_1 d$
s scale
1 = 1000 Å

Fig. 19.

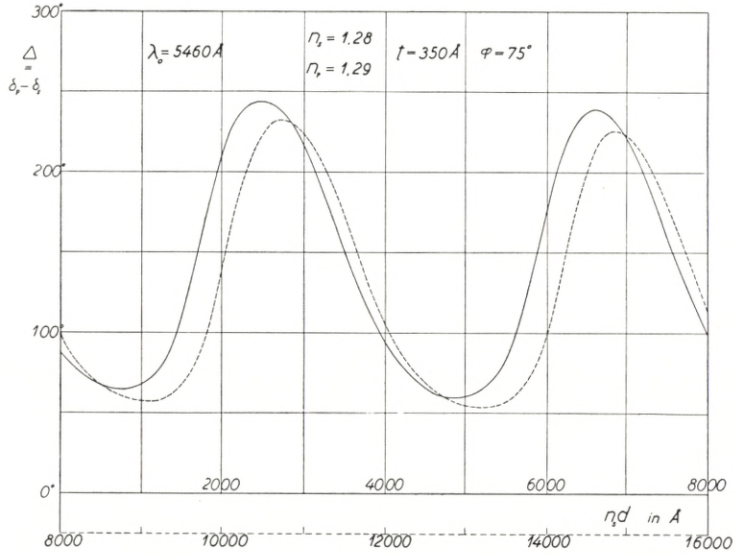
$\Delta = \delta_p - \delta_s$
$\lambda_0 = 5460\,Å$
$n_1 = 1.28$
$n_2 = 1.29$
$t = 350\,Å$
$\varphi = 75°$
300°
200°
100°
0°
2000
4000
6000
8000
8000
10000
12000
14000
16000
$\eta_1 d$ in Å

Fig. 20.

With the apparatus now in use $\lambda_m^{(v)}$ can be measured with a spectroscope (at normal incidence) before air (and H_2O) is admitted to the vacuum chamber.

We have

$$m\lambda_m^{(v)} = 2\, n_s^{(v)} \cdot d + Z(\lambda_m^{(v)},\ n_s^{(v)}). \qquad (4,\ 6)$$

$Z(\lambda_m^{(v)},\ n_s^{(v)})$ can approximately be calculated from ([A] fig. 8) when the λ-scale is transformed. If $\varkappa(\lambda)$ has the value adapted in [A], the observed value of $\lambda_m^{(v)}$ should be equal to the value calculated from (4, 6).

From the observed values of $\lambda_m^{(v)}$ and $\lambda_m^{(A)}$ it is possible to determine $n^{(A)}$ from (4, 4) and (4, 6). As $Z^{(v)} \simeq Z^{(A)}$, we approximately obtain:

$$\lambda_m^{(A)} - \lambda_m^{(v)} = \frac{n^{(A)} - n_s^{(v)}}{n^{(A)}} \left(\lambda_m^{(A)} - \frac{Z(\lambda_m^{(A)},\ n^{(A)})}{m} \right), \qquad (4,\ 7)$$

i. e. the shift in wavelength of the transmission band towards red is proportional to the wavelength especially for filters of higher orders m. For MgF_2 we have very nearly $n^{(v)} = 1.28$ and a shift of $\lambda_2^{(A)} - \lambda_2^{(v)} = 400$ Å is observed when $\lambda_2^{(A)} = 6560$ Å. From (4, 7) we then get $n^{(A)} = 1.365$.

Especially for filters of smaller area (5×5 cm) a cover glass is cemented upon the thin filter layers for protection. The cement most commonly used is a balsam or better a plastic dissolved in xylene or toluene. If porosities are present in the fluoride layer, the cement will fill the pores and a further shift from $\lambda_m^{(A)}$ to $\lambda_m^{(C)}$ towards the red will result. For cryolite quickly evaporated this shift turns out to be as great as $\lambda_2^{(C)} - \lambda_2^{(A)} \simeq 350$ Å ($\lambda_2^{(A)} = 6560$ Å), but here $\lambda_2^{(A)} - \lambda_2^{(v)} = 100$ Å only; however, these shifts are rather unpredictable. For MgF_2 the shift $\lambda_2^{(C)} - \lambda_2^{(A)}$ is only 50—150 Å, but unfortunately this shift seems to be more dependent upon the conditions of evaporation than $n^{(v)}$ and $\lambda_m^{(A)} - \lambda_m^{(v)}$ do. So far experiments seem to show that $n^{(v)}$ is only slightly dependent upon pressure, when this is lower than 10^{-4} mm *Hg*, but is dependent upon the temperature of the crucible ("molybdenum boat"). The higher the temperature the higher $n^{(v)}$ (or the higher $n_p^{(v)} - n_s^{(v)}$) becomes and $\lambda_m^{(C)} - \lambda_m^{(A)}$ becomes smaller, but $\lambda_m^{(A)} - \lambda_m^{(v)}$ will be nearly the same. Recent investigations seem to indicate that this dependence upon the temperature

of the crucible is partly due to impurities in the MgF_2 used and all the above properties, which are so important when making interference filters, require much more experimental investigation with uncontaminated MgF_2 powder.

An alternative determination of $n^{(A)}$ or $(n_s^{(A)}, n_p^{(A)})$ can according to ([A] p. 39—45) be made from observation of $(\lambda_m^{(s)}, \lambda_m^{(p)})$ at an oblique angle of incidence.

In fig. 21 and fig. 22 $(\delta_p, n_s d)$ and $(\delta_s, n_s d)$ curves are shown which are calculated for $n_s = 1.28$, $n_p = 1.285$ and $\lambda_0 = 5460$ Å $(\nu - i\varkappa = 0.1 - i\,3.5)$. The solid curves correspond to $t = 500$ Å and the dotted curves to $t = 200$ Å for the basic silver layer.

Fig. 23 and fig. 24 show the ratios between the s and p circles employed at the construction of figs. 21—22.

Figs. 25—26 are quite analogous to figs. 21—22, but calculated for $\lambda_0 = 7400$ Å $(\nu - i\varkappa = 0.1 - i\,5.0)$. When a red-infrared sensitive photocell is used as reciever in the polarimeter, the application of λ_0 for this spectral region has many advantages because of the optimum conditions for silver layers in this region.

Small changes in the constants from n_s, n_p, λ_0 to n_s', n_p', λ_0' can be compensated for in the figs. 21—22 and 25—26 by transforming the $n_s d$ scales to $(n_s d)' = n_s d \cdot \dfrac{n_p' \cdot \lambda_0 \cdot \cos \chi_p'}{n_p \cdot \lambda_0' \cdot \cos \chi_p}$ (p component) and analogous for the s component.

In fig. 27 the $(\Delta, n_s d)$ curves are constructed from figs. 21—22 (solid curve) and from figs. 25—26 (dotted curve) in the case of $t = 500$ Å $\lambda_m^{(A)}$ and $\lambda_m^{(v)}$ scales calculated from (4, 4—6) and ([A] fig. 8) are added. However, it should be emphasized that fig. 27 may only be regarded as a first approximation. Experiments with uncontaminated MgF_2 powder will be continued for a more accurate determination of n_p and n_s.

From fig. 27 it is apparent that all thicknesses nd up to 6000 Å can be controlled with great accuracy (better than 10 Å), when the conditions of the evaporation process are constant).

In fig. 28 two (Δ, nd) curves have been constructed for $n_p = n_s = 1.29$. $\lambda_0 = 5460$ Å for the solid line curve $(\nu - i\varkappa = 0.1 - i\,3.5)$ and $\lambda_0 = 6560$ Å for the dotted line curve $(\nu - i\varkappa = 0.1 - i\,4.3)$ and $t = 350$ Å for both curves. For a filter of the second order we obtain for a definite $n_s d$, a value of Δ (for $\lambda_0 = 5460$ Å) in fig. 28 which is near the value for Δ we obtain from fig. 27,

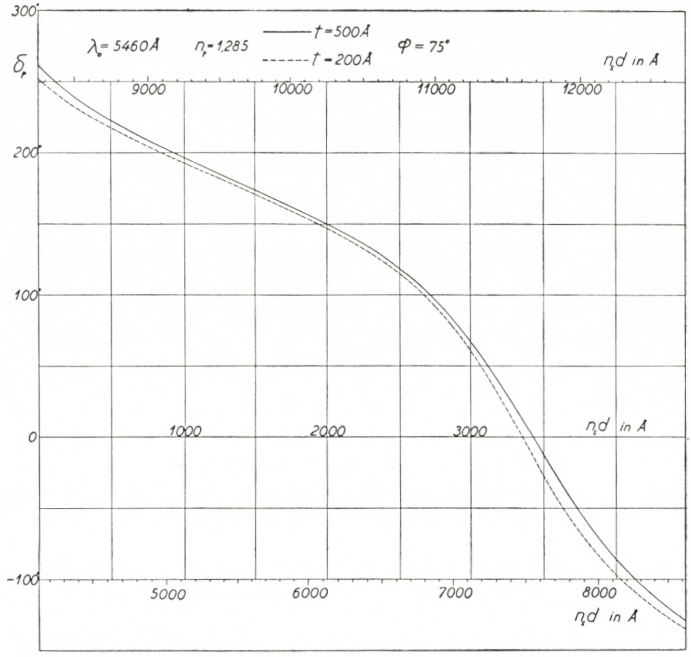
$\lambda_0 = 5460\,Å$
$n_r = 1{,}285$
$t = 500\,Å$
$t = 200\,Å$
$\varphi = 75°$
δ_r
$n_r d$ in Å
300
200
100
0
-100
9000
10000
11000
12000
1000
2000
3000
5000
6000
7000
8000

Fig. 21.

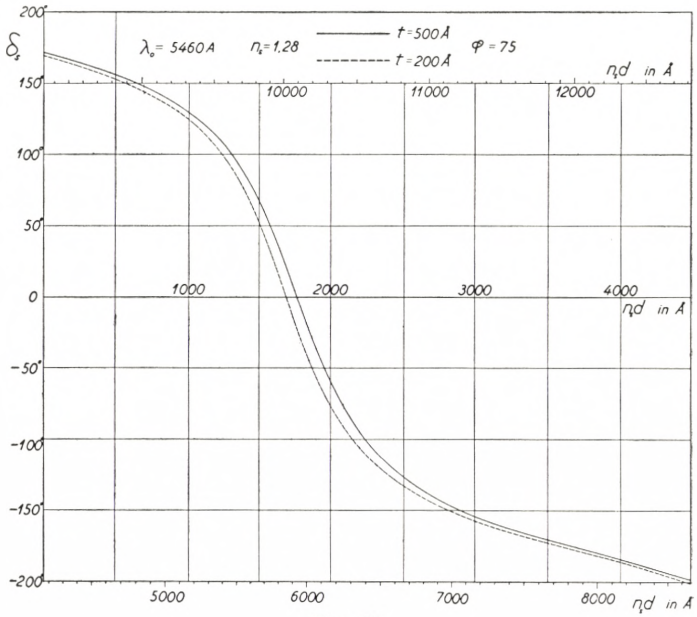
$\lambda_0 = 5460\,Å$
$n_s = 1{,}28$
$t = 500\,Å$
$t = 200\,Å$
$\varphi = 75$
δ_s
$n_s d$ in Å
200
150
100
50
0
-50
-100
-150
-200
10000
11000
12000
1000
2000
3000
4000
5000
6000
7000
8000

Fig. 22.

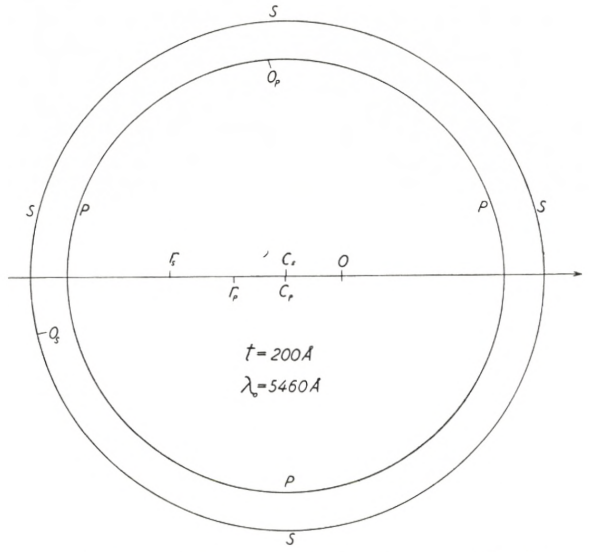

Fig. 23. Proportion between s and p circles for $t = 200$ Å $0_s = (\varrho_s, \delta_s)$ and $0_p = (\varrho_p, \delta_p)$ for the silver layer.

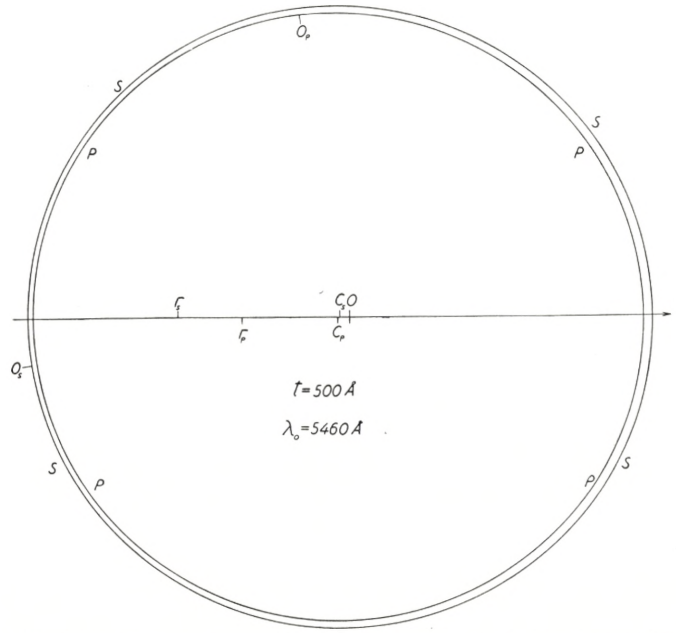

Fig. 24. Proportion between the s- and the p-circle when $t = 500$ Å.

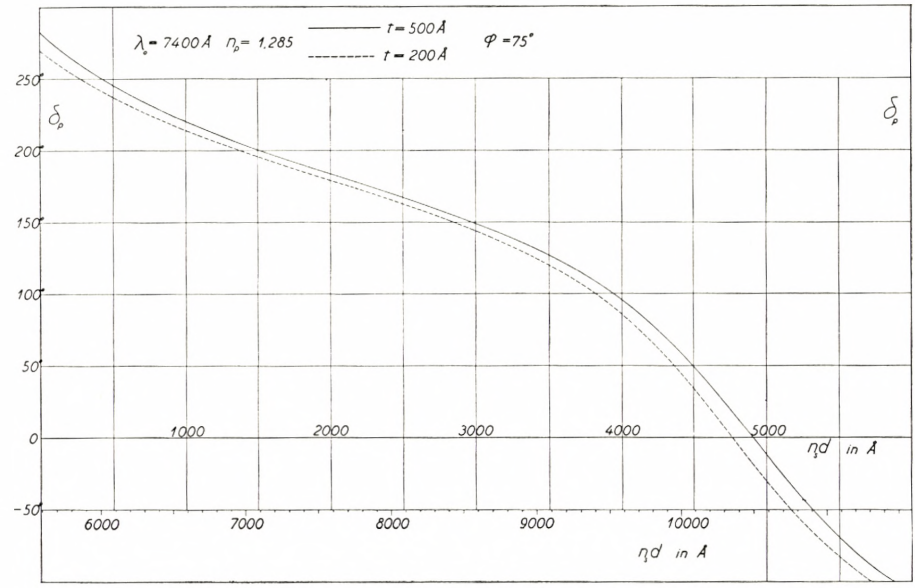
λ₀ = 7400 Å n_p = 1,285
t = 500 Å
t = 200 Å
φ = 75°
δ_p
δ_p
250°
200°
150°
100°
50°
0
-50°
1000
2000
3000
4000
5000
η_p d in Å
6000
7000
8000
9000
10000
η_p d in Å

Fig. 25.

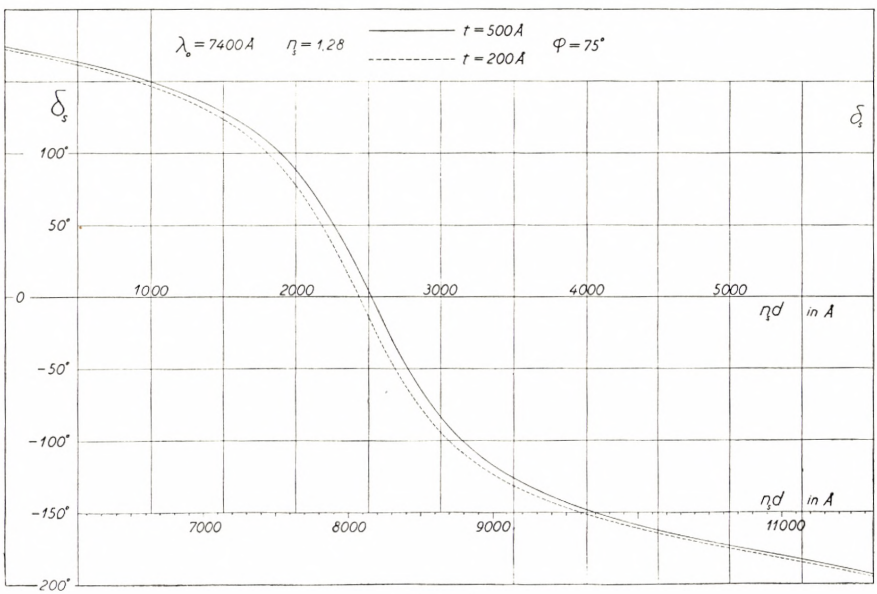
λ₀ = 7400 Å η_s = 1,28
t = 500 Å
t = 200 Å
φ = 75°
δ_s
δ_s
100°
50°
0
-50°
-100°
-150°
-200°
1000
2000
3000
4000
5000
η_s d in Å
7000
8000
9000
11000
η_s d in Å

Fig. 26.

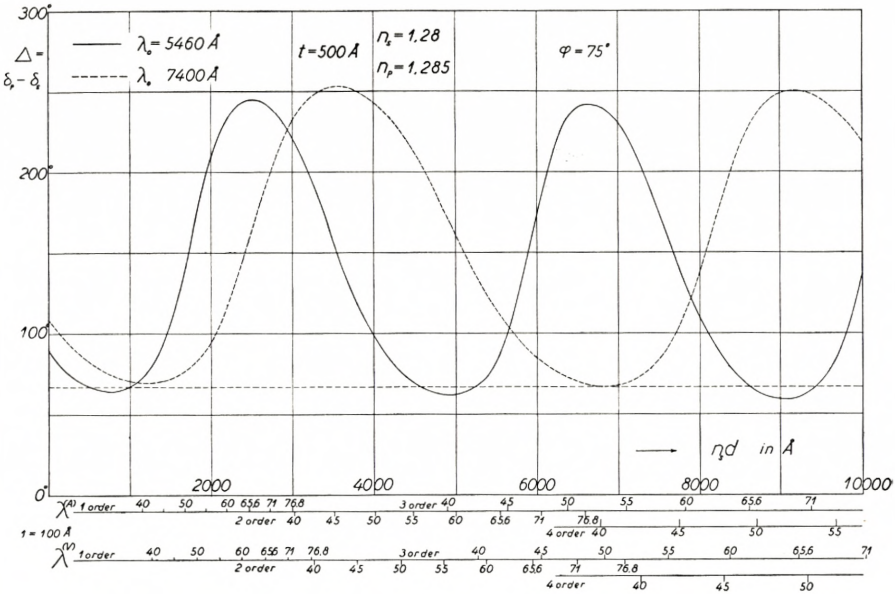
300°
Δ = δ_r − δ_i
λ_o = 5460 Å
λ_e 7400 Å
t = 500 Å
n_e = 1,28
n_p = 1,285
φ = 75°
200°
100°
0°
nd in Å
2000
4000
6000
8000
10000
λ(A) 1 order 40 50 60 65,6 71 76,8
2 order 40 45 50 55 60 65,6 71
3 order 40 45 50 55 60 65,6 71
4 order 40 45 50 55
1 = 100 Å
λ(V) 1 order 40 50 60 65,6 71 76,8
2 order 40 45 50 55 60 65,6 71 76,8
3 order 40 45 50 55 60 65,6 71
4 order 40 45 50

Fig. 27.

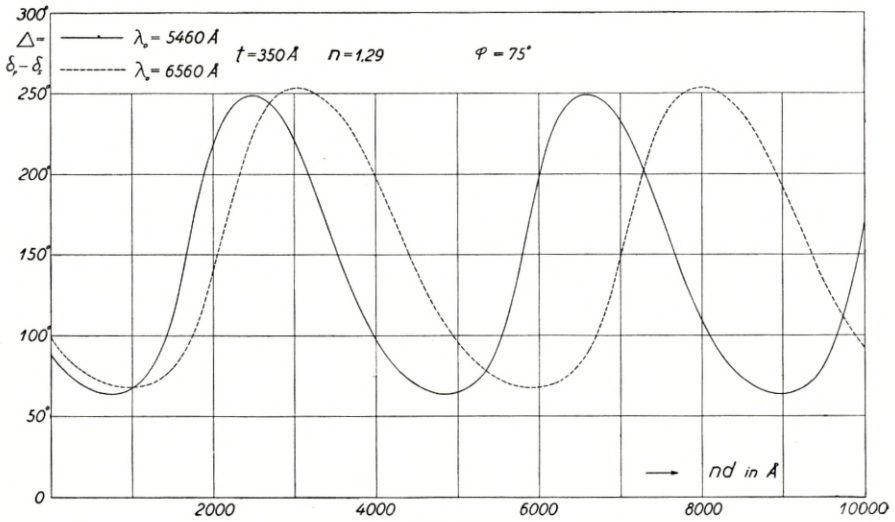
300°
Δ = δ_r − δ_i
λ_o = 5460 Å
λ_o = 6560 Å
t = 350 Å
n = 1,29
φ = 75°
250°
200°
150°
100°
50°
0
nd in Å
2000
4000
6000
8000
10000

Fig. 28.

i. e. if it is assumed that there is no birefringence and n is determined from measurement of $\lambda_m^{(v)}$, we obtain too high a value.

Figs. 27—28 further shows that when three different values of λ_0 are available, also values of $n_s \cdot d$ higher than 6000 Å can be controlled with great accuracy.

At the control of nd only Δ is used. However, also ψ is observed

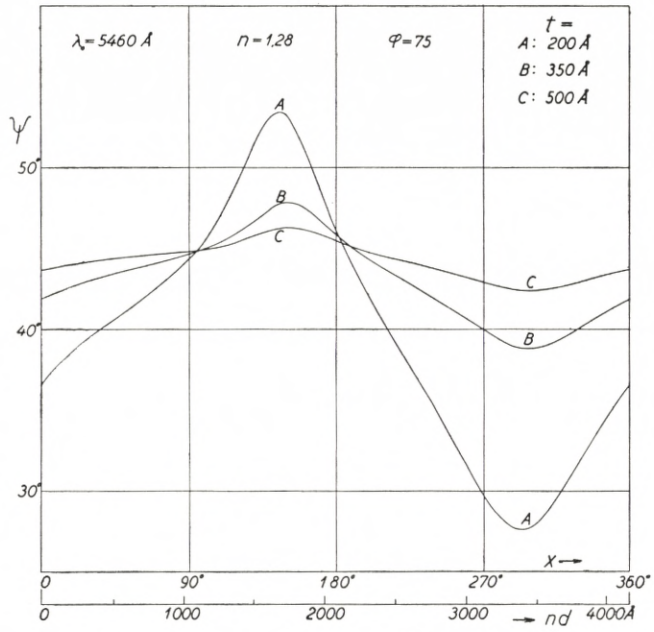

Fig. 29. ψ calculated for different thicknesses t of the basic silver layer. $\operatorname{tg} \psi = \frac{\varrho_p}{\varrho_s}$.

by analyzing the elliptically polarized light reflected from the silver-dielectric layers (fig. 2). Fig. 29 shows (ψ, x) or (ψ, nd) curves all calculated for $n = 1.28$ and for different thicknesses t of the basic silver layer. As opposed to Δ, ψ shows a strong dependence upon t and ν for the basic silver layer. $\psi_{\max} - \psi_{\min}$ can be used for a determination of t if ν is known and at $t = \infty$ be used for a determination of ν, which is independent of small errors in the polarimeter adjustment.

§ 5. Control of the Dielectric Layers for Compound Filters $M'L_{2m}M''L_{2m}M'$ and $M'L_{2m}M''L_{2p}M''L_{2m}M'$.

For these types of filters the polarimetric method for control will be especially well suited because all the measurements take place in *reflected light* and on the filter base itself and because reflection from M', M'' or from the combinations $M'\,L_{2m}M''$ and $M'\,L_{2m}M''\,L_{2p}M''$ (as basic layers for the dielectric layers) result in about the same value for Δ and δ_s (if λ_0 not corresponds to a transmission band for the basic interference filter at $\varphi = 75°$) and the $(\Delta,\ nd)$ curves above (for $t = 500$ Å) can still be used.

As briefly mentioned above the most direct method of control, for a filter of the second or higher order will be to chose the wavelength of the polarimeter light λ_0 in such a way that the evaporation has to be stopped at a value of Δ in the neighbourhood of Δ_0 corresponding to one or more total periods of the $(\Delta,\ nd)$ curve ($\lambda_0 = 2\,dn\cdot\cos\chi$ or $\lambda_0 = dn\cdot\cos\chi$).

Below a table is added which gives λ_0 for filters of the second order (1 period) and of the third order (2 periods) for different values of $\lambda^{(A)}$.

TABLE 9.

$\lambda^{(A)}$	λ_0 $M''L_4M''$	λ_0 $M''L_6M''$
4000 Å	4060 Å	
4500	4730	
5000	5400	4270 Å
5500	6060	4760
6000	6710	5240
6560	7430	5780
7100	8100	6290
7680	8840	6840

In this case the control is independent of the composition of the basic system of layers. In the case where this system consists of a filter $M'\,L_4M''$, as shown in fig. 30 A, $(\Delta,\ \psi)$ of light reflected from A will be the same as $(\Delta,\ \psi)$ for light reflected from a silver layer with thickness $t' + t''$ (fig. 30 B) if $n - i\,\varkappa$ is the same for the three silver layers.

The small birefringence present acts as if $n \cdot \cos \chi$ is greater than in reality. Table 9 is calculated in such a way that $\lambda^{(A)} = 6560$ Å (third order) corresponds to the value of λ_0 actually measured.

When we wish to make a filter $M' L_{2m} M'' L_{2m} M'' L_{2m} M'$ it should further be noted that $n^{(A)} \cdot d$ for the central layer is different from $n^{(A)} \cdot d$ for the outer dielectric layers, as the filters $M' L_{2m} M''$ and $M'' L_{2m} M''$ shall have the same value for $\lambda_m^{(A)}$. The $n_s^{(v)} \cdot d$

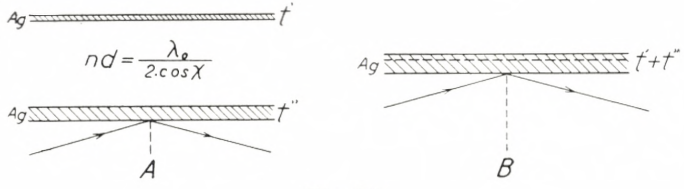

Fig. 30.

values to be used on the $(\Delta, n_s d)$ curve are calculated from (4, 5). The differences betweens the $n_s^{(v)} d$ values for the central and the outer layers vary from about 15 Å at $\lambda_m^{(A)} = 4000$ Å to 115 Å at $\lambda_m^{(A)} = 7700$ Å.

§ 6. Control of the Dielectric Layers for Filters where *L* and *H* Layers are Added to the Silver Layers.

Also at this type of filters (the theory of which is given in ([A] § 6)) all the dielectric layers can be controlled on the filter base itself (fig. 31).

The calculation of the (Δ, nd) curve is carried out graphically by means of a polar coordinathograph (see fig. 7).

As an example fig. 32 shows the (Δ, nd) curve calculated for the simplest filter of this type $M L' H_2 L' M$ in such a way that

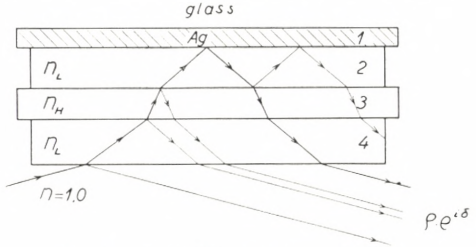

Fig. 31. $ML' HL$ system of layers.

peak transmission occurs at $\lambda = 6560$ Å. Here $\lambda_0 = 5460$ Å will give sufficient accuracy by control of all the dielectric layers, but in most cases (in the case of more complicated filters of this type)

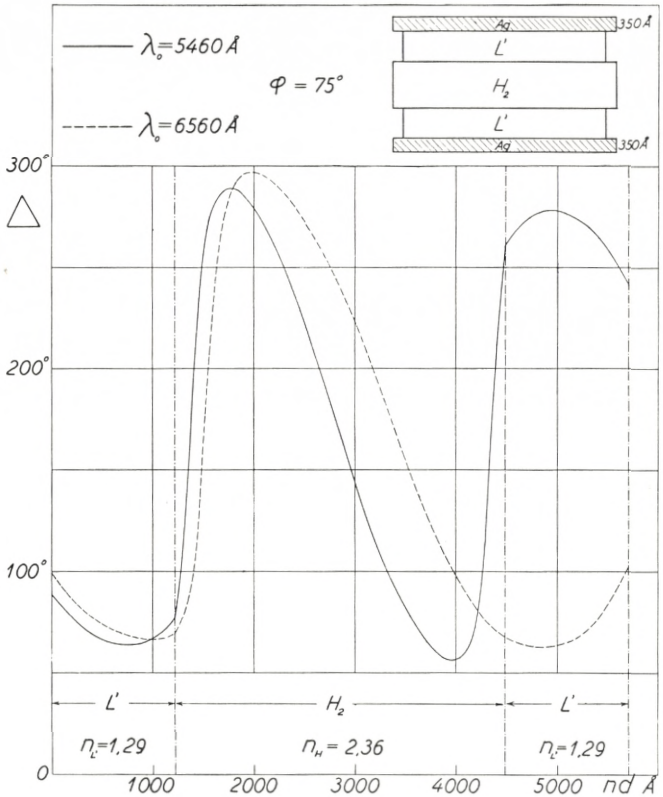

Fig. 32.

the calculation has to be repeated for another value of λ_0 to be able to control all the dielectric layers with sufficient accuracy.

The control of a high-index layer is much easier than for a low-index layer as $n_H^{(v)} = n_H^{(A)} = n_H^{(c)}$ and because of the small value of $\Delta\lambda_1$ (Table 1).

In fig. 32 it is assumed that $n_H = 2.36$ $n_L^{(v)} = 1.29$ and $n^{(A)} = 1.37$.

§ 7. Thickness Control in the Production of All-Dielectric Filters.

As mentioned above, the usual procedure employed for this type of filters is measurement of the intensity $R(d)$ in *reflected* monochromatic light at normal incidence from test plates; at least two test plates are used, one for the low- and the other for the high-index layers. In fig. 33 $R(d)$ is calculated for the test plate with the low-index layer ($n_L^{(v)} = 1.29$, MgF_2) and in fig. 34 $R(nd)$ for the test plate with the high-index layer ($n_H = 2.36$, ZnS). By change of wavelength λ_0 or by measuring the difference $R_1 - R_2$ corresponding to two different wavelengths as indicated in figs. 33—34 it will be possible to control nd for all the layers with an accuracy of about 30 Å (if photocells and an amplifier are used). It should further be mentioned that JACQUINOT and GIACOMO [4] have constructed an apparatus which enables them to measure the derivative $\frac{dR}{d\lambda_0}$ (which can be used for thickness control with great accuracy for thicknesses where $R(d)$ has a maximum or a minimum).

This rather simple test plate procedure offers good results by production of filters of smaller areas. [2] However, as mentioned above, the filter base in the case of production of filters of larger areas must be rotated during evaporation and the test plates placed perpendicularly above the evaporation source and far from the filter base. In this case the test-plate procedure for control would be rather uncertain, and for this reason it would be desirable to control all the filter layers (and especially the 3—5 central layers) on the filter base itself. In the case of this type of filters this is also possible by means of the polarimetric method and with higher accuracy than obtained with the testplate method.

The (Δ, nd) and (ψ, nd) curves are calculated by means of the graphical procedure shown in fig. 7 p. 9.

Such a construction is shown in figs. 35—36. $n_L^{(v)} = 1.29$ and $n_H = 2.36$. λ_0 has been chosen in such a way that $x_H = 180 \cdot \frac{\lambda_1}{\lambda_0} \cdot \cos \chi_H$ is equal to 180° i. e. $\frac{\lambda_1}{\lambda_0} = 1.096$. ($\varphi = 75°$).

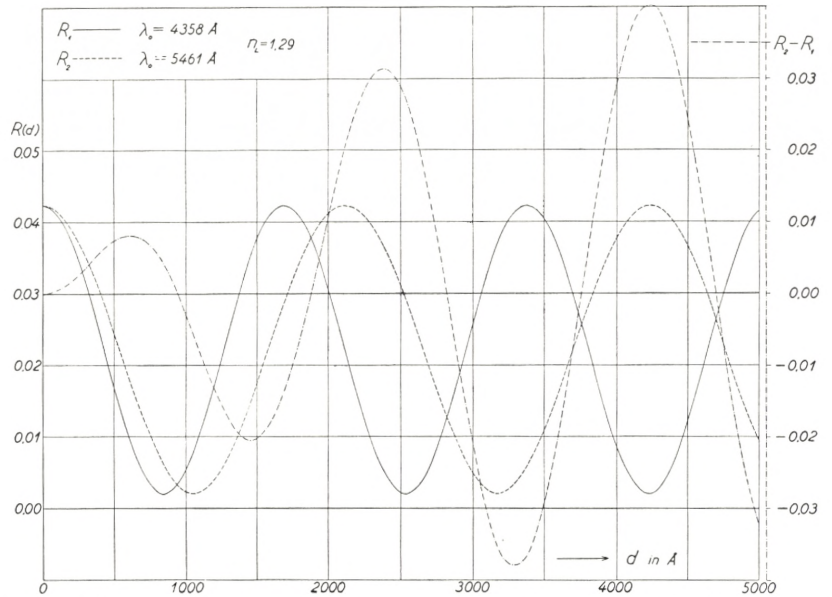

Fig. 33. $R\,(d)$ from a glass surface with $n = 1.518$ coated with a MgF_2 film ($\varphi = 0$).

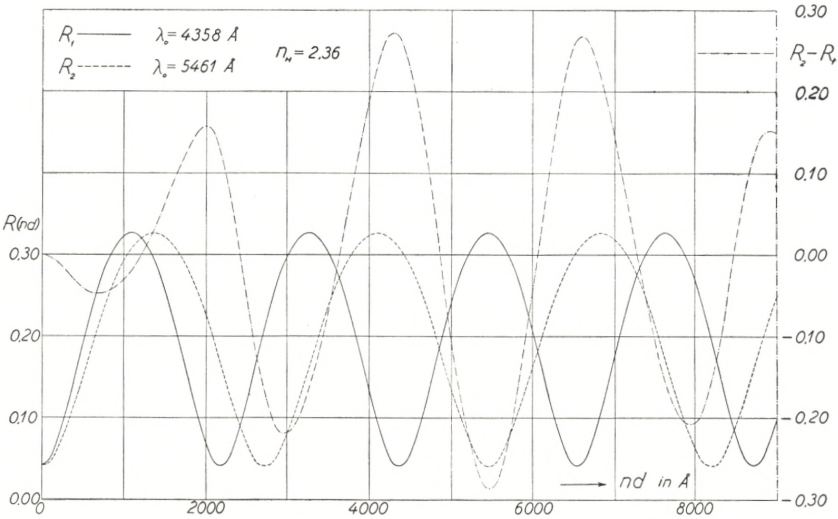

Fig. 34. $R\,(nd)$ from a glass surface with $n = 1.518$ coated with a ZnS film ($\varphi = 0$).

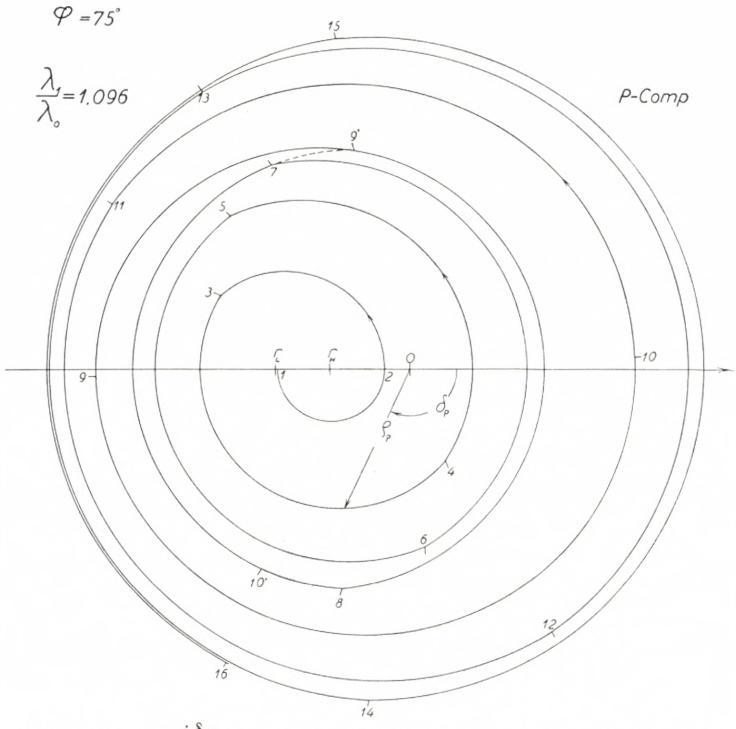

Fig. 35. $\varrho_p \cdot e^{i\delta p}$ during the build-up of the filter $D_7\, L_2\, D_7$.

$x_L = 180 \cdot \dfrac{\lambda_1}{\lambda_0} \cdot \dfrac{n_L^{(v)}}{n_L^{(A)}} \cdot \cos \chi_L$ and when $\dfrac{n_L^{(v)}}{n_L^{(A)}} = 0.9377$ we have $x_L = 122°.62$ ($x_H = x_L = 180°$ for $\lambda = \lambda_1$ and $\varphi = 0$).

Fig. 35 shows (ϱ_p, δ_p) and fig. 36 (ϱ_s, δ_s) (in polar coordinates) for the filter $D_7 L_2 D_7$ as the layers grow simultaneously.

The numbers 1—16 on the spirals denote the values of (ϱ, δ), where the evaporation has to be interrupted and a change to the other dielectric material to take place. E. g. the number 8 means (ϱ, δ) in reflection from the seven layers $D_7 = HLHLHLH$ (1 means (ϱ, δ) for the uncoated glass plate), 9 means reflection from $HLHLHLHL_2$, etc. As $x_H = 180°$, the same construction can be used for the filter $D_8 H_2 D_8$. The number 9′ in figs. 35—36 means (ϱ, δ) corresponding to reflection from the system $D_8 = HLHLHLHL$ (and 10′ in fig. 35 means reflection from D_9; in fig. 36, 10′ is equal to 8).

From figs. 35—36 the corresponding (Δ, nd) and (ψ, nd)

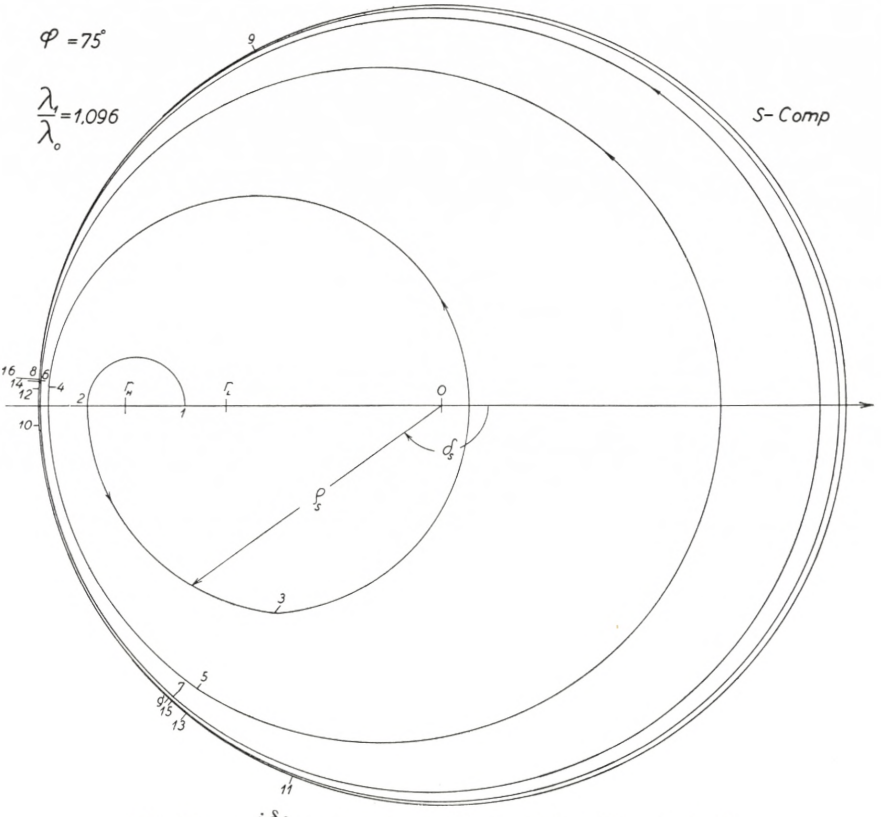

Fig. 36. $\varrho_s \cdot e^{i\delta s}$ during the build-up of the filter $D_1\, L_2\, D_7$.

curves can be constructed (not given here). The positions of the points on the (Δ, nd) curve which correspond to the H and L layers would be still better if λ_0 was chosen still smaller than λ_1 e. g. $\frac{\lambda_1}{\lambda_0} = \frac{6560}{5461} = 1.20$. Unfortunately λ_0 can not be chosen higher than or equal to λ_1, as in this case $\frac{\varrho_p}{\varrho_s}$ would be too low to enable an accurate measurement of Δ.

Another procedure by polarimetric control would be to measure the difference $\Delta(\lambda_0) - \Delta(\lambda_0')$ in Δ corresponding to two neighbouring wavelengths λ_0 and λ_0' (e. g. 5461 Å and 5893 Å). When this difference is measured with an accuracy of 5′ (five minutes of arc) a sufficiently accurate control would be possible for values of nd where Δ has a maximum or a minimum.

Summary.

A polarimetric method for thickness control in the production of interference filters has been treated in detail.

Plane-polarized light with wavelength λ_0 is reflected from the filter layers at an oblique angle of incidence ($\varphi = 75°$) and thus becomes elliptically polarized. λ_0 is chosen in such a way that measurement of $\Delta = \delta_p - \delta_s$ for the elliptically polarized light determines the thickness of a dielectric layer with an accuracy better than 10 Å (when conditions during the evaporation process are constant).

This method of control, which follows the growth of the dielectric layer on the filter base itself, can be applied to all types of interference filters (also reflection interference filters) and is especially well suited for control of the dielectric layers for filters of the types $ML_{2m}M$, $M'L_{2m}M''L_{2m}M'$ and $M'L_{2m}M''L_{2p}M''L_{2m}M'$.

A (Δ, nd) curve for a filter $ML_{2m}M$ can be constructed from measurements of (Δ_0, ψ_0) for the silver layer M first evaporated and from measurements of Δ_{max} and Δ_{min} during evaporation; and the value of Δ at which the evaporation is to be stopped can be calculated corresponding to a definite wavelength for the transmission band λ_m of the filter.

A small birefringence ($n_p - n_s \simeq 0.005$) is present for an evaporated fluoride layer (cryolite or MgF_2) and the index of refraction for rapidly evaporated MgF_2 is much lower in vacuum ($n^{(v)} = 1.28$) than in air ($n^{(A)} = 1.365$). Furthermore measurements of (Δ_0, ψ_0) for silver layers show that $\varkappa$ for a silver layer of the thickness employed for interference filters is different from $\varkappa$ for an opaque silver layer.

The experiments will be continued in order to obtain more refined information about $n_p(\lambda)$ and $n_s(\lambda)$ (in vacuum and air) for thin evaporated MgF_2 films.

Acknowledgement.

These investigations have been carried out at the Physics Department of the Royal Veterinary and Agricultural College, Copenhagen.

I wish to express my gratitude to the Director af the Physics Department, Professor EBBE RASMUSSEN, for the great interest he has taken in this work.

Physics Department
Royal Veterinary- and Agricultural College
Copenhagen.

References.

(*A*) ALFRED HERMANSEN, A Theory of Interference Filters, Dan. Mat. Fys. Medd. **29,** No. 13 (1955).
(1) K. M. GREENLAND and C. BILLINGTON, Proc. Phyc. Soc. B, **63,** 359 (1950) or J. Phys. et le Radium **11,** 419 (1950).
(2) CH. DUFOUR, Le Vide, No. 16—17, 480 (1948) or Theses (Paris 1950).
(3) P. JACQUINOT et P. GIACOMO, J. Phys. et le Radium **13,** 59 A (1952).
(4) A. HERMANSEN, Nature **167,** 104 (1951).
(5) P. DRUDE, Ann. d. Phys. und Chem. **36,** 865 (1889).
— ibid. **39,** 481 (1890).
(6) ANTONIN VAŠÍČEK, J. Opt. Soc. Am. **37,** 145 (1947) and ibid. **37,** 979 (1947).
(7) ALEXANDRE ROTHEN, Rev. Sci. Instr. **16,** 26 (1945).
(8) ALEXANDRE ROTHEN and MARJORIE HANSON, Rev. Sci. Instr. **19,** 839 (1948).
— — ibid. **20,** 66 (1949).
(9) A. HERMANSEN, Nature, **174,** 218 (1954).
(10) JØRGEN RYBNER and K. STEENBERG SØRENSEN, Table for Use in The Addition of Complex Numbers (Jul. Gjellerups forlag, København 1948).
(11) P. COTTON, J. Phys. et le Radium **11,** 321 (1950).
(12) MAX BORN, Optik (1933) (Berlin, Verlag von Julius Springer).
(13) B. H. BILLINGS, J. Opt. Soc. Am. **40,** 471 (1950).

Indleveret til selskabet den 25. april 1955.
Færdig fra trykkeriet den 24. september 1955.